

AD-A142 409

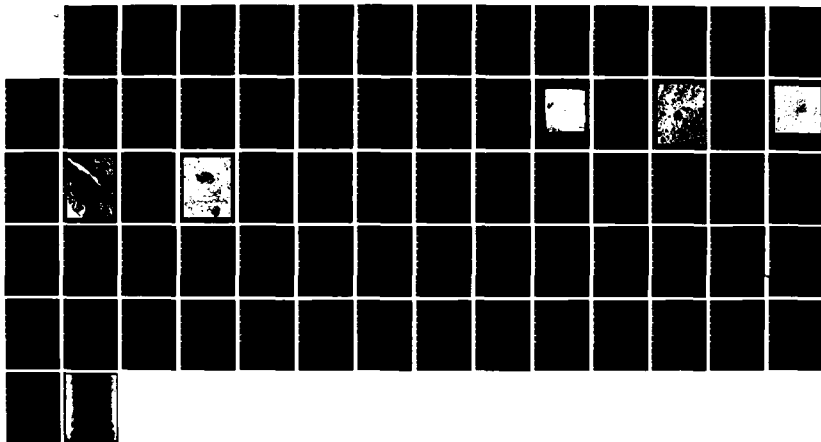
METEOROLOGICAL RESEARCH AND SUPPORT FOR THE MIZEX
(MARGINAL ICE ZONE EXPERIMENT) PROGRAM(U) AIRBORNE
RESEARCH ASSOCIATES WESTON MA R MARKSON 04 APR 84
N00014-83-C-0088

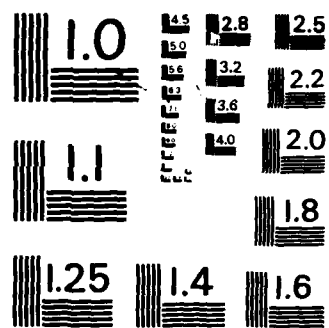
1/1

UNCLASSIFIED

F/G 4/2

NL





MICROCOPY RESOLUTION TEST CHART
NATIONAL BUREAU OF STANDARDS-1963-A

AD-A142 409

METEOROLOGICAL RESEARCH AND
SUPPORT FOR THE MIZEX PROGRAM

FINAL REPORT

by

Ralph Markson

Airborne Research Associates
46 Kendal Common Road
Weston, Massachusetts 02193
(617)899-1834

to

Office of Naval Research
Polar Program (Code: 425AR)
Mr. Charles Luther, Scientific Project Monitor

CONTRACT NO. N00014-83-C-0088

DTIC

APPROVED FOR PUBLICATION
DISTRIBUTION STATEMENT

JUN 20 1984
[Handwritten signature]

4 April 1984

DTIC FILE COPY

84 06 20 052

CONTENTS

A. Introduction..... Page 1

B. Meteorological Research..... 1

1. Objectives..... 1

2. Instrumentation..... 3

3. Determination of fluxes..... 4

4. Operational factors..... 4

5. Flights from Longyearbyen..... 5

6. Personnel..... 6

7. Examples from preliminary data analysis..... 6

C. Photography..... 7

D. Availability of Data..... 8

E. References..... 9

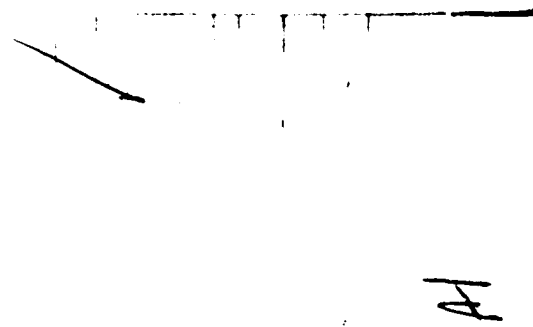
Table I: Summary of MIZEX-83 Flights by ARA Baron

Table II: Summary of meteorological observations from Baron measurements during MIZEX-83

Figures: 1-3

Pictures: 1-5

Appendix A: Catalog of 38 temperature and humidity vertical profiles.



A Introduction

This report will discuss the measurements and ice photography obtained from the Beechcraft Baron atmospheric research aircraft operated by Airborne Research Associates (ARA) during the 1983 Marginal Ice Zone Experiment (MIZEX-83). The aircraft was instrumented to measure the bulk meteorological parameters, turbulence, surface fluxes (inferred), sea surface temperature the atmospheric electric field and conductivity. In addition, photography was obtained including the only photomosaic in MIZEX-83 and several transects which were made in color. Eleven flights were conducted from the Longyearbyen airport; one was for the mosaic and the others were for meteorology. The flight program was successful both in obtaining a 40 km x 40 km photomosaic of the region studied by the remote sensing aircraft on 11 July and in obtaining good quality meteorological data almost all the time. All flights were accomplished despite the fog, low ceilings and minimal visibility because it was possible to operate just above the ice/ocean surface. The meteorological measurements were mostly concerned with the evolution of the planetary boundary layer under conditions of on-ice and off-ice winds. Measurements were made using horizontal and vertical profile flight patterns. While the aircraft measurements were an integral part of the meteorological program, the drag coefficients and flux measurements should be useful in other MIZEX investigations concerned with ice and oceanography. The meteorological measurements are being analyzed by C W Fairall at Pennsylvania State University. To date only a limited amount of data analysis has been accomplished; this work will be completed during the next year. Arrangements will be made to distribute photographic imagery to MIZEX and other interested scientists. This report will describe the meteorological and photographic data that is available.

B Meteorological Research

1 Objectives. Observational descriptions emphasized in characterizing atmospheric forcing of the marginal ice zone (MIZ) are in most respects completely opposite of those descriptions emphasized in land-atmosphere and/or sea-atmosphere large scale experiments. This is because locations for the latter are chosen to minimize the role of horizontal variations of the boundary conditions. The goal of such descriptions is to relate large scale quasi-permanent features of the atmosphere as influenced by regional continental (ice cap) features to mesoscale spatial and temporal features. This requires that the experimental observations include horizontal and vertical measurement of the parameters used to determine the fluxes of momentum, heat and moisture.

It is important that the atmospheric forcing fields be known for 100 to 200 km from the immediate experimental area (ice edge). Ice motion and ocean eddies at the edge clearly respond to atmospheric forcing on this scale. Estimates of the flux fields

can be made from large scale (300 km) fixed point pressure and temperature measurements using existing synoptic scale planetary boundary layer (PBL) models. However, scaling of the transfer from the large to small scale features is required. Present scaling procedures appear to range from good for the surface layer to poor for the inversion region. The latter requires turbulence measurements in three dimensions.

The need for horizontal and vertical descriptions of relevant atmospheric properties in the MIZ has led to the consistent inclusion of aircraft measurements in experimental plans and the data acquisition capabilities of the ARA Baron provided the measurements required for most of the objectives. They consist of both intermittent horizontal and vertical descriptions which can be related to the continuous fixed point observations obtained from shipboard and icepack locations. Thus they make possible study of the relationships between the synoptic scale wind field and the turbulent transfer of momentum and the synoptic scale temperature and humidity fields and their surface layer fluxes.

The long term objective of the measurements was to provide data which will facilitate the creation of models for relating large scale atmospheric features, discernible from synoptic scale pressure fields and satellite imagery, to surface layer forcing of the ice upper ocean region of the MIZ.

The short term objectives were to obtain horizontal and vertical descriptions of the following atmospheric properties and relate them to coincident fixed point surface measurements. The descriptions are of the:

(a) momentum, sensible and latent heat fluxes determined from dissipation measurements based on small scale turbulence properties,

(b) water vapor content and cloud liquid water content which determine the long and short wave radiation fluxes, and,

(c) surface and inversion features determining boundary conditions for vertical transfer of scalar and vector properties. These features would include percentage of ice/water **coverage**, surface temperature and inversion gradients.

From an ice/sea science perspective, the above objectives can be considered in view of the complex system being studied. The ice/sea-atmospheric interface is bordered by the atmospheric turbulent mixed layer extending upward from 50-500 meters, in which the source of turbulent energy is the velocity and buoyancy gradients created by interactions at the interface. The mixed layer couples the large scale features of the troposphere to the interface. The mixed layer interacts with the upper layer (troposphere) at the inversion transition region by means of turbulent forcing entrainment.

The above description indicates that the evolution of the momentum, density and turbulence of the forcing atmospheric boundary layer is a result of processes at both the surface and inversion regions. Properties at both regions vary in the horizontal in the MIZ. A source or sink of energy in the atmospheric boundary layer which can not be neglected is radiation. Both long and short wave (solar) radiation fluxes into the surface are critically dependent on the existence of aerosols and cloud within the mixed layer.

2. Instrumentation. The following is a list of parameters and methods of measurement utilized on the Baron aircraft

(a) Air temperature--standard Rosemont 50 ohm resistance wire sensor.

(b) Dew point temperature--Cambridge dew point system utilizing a chilled mirror.

(c) C_T^2 temperature structure function--determined from rms temperature differences between two 5 micron diameter tungsten wires on a vertical mast at the wingtip. Two separate electronic systems and antenna arrays are utilized for redundancy in case a wire breaks in flight. The probes can be retracted and extended in flight to protect them from breakage when flying through ice crystals.

(d) ϵ eddy dissipation rate of kinetic energy--measured with a 5 micron diameter tungsten hot wire anemometer in a constant temperature circuit. The signal is bandpass filtered, squared and average. The C_T^2 and ϵ wires can be interchanged in flight.

(e) C_q^2 humidity structure function parameter--measured with a Lyman-alpha instrument and electronic signal processing.

(f) SST, sea surface temperature--measured with a Barnes PRT-5 infra-red radiation thermometer.

(g) Airspeed--measured with a Rosemont pressure transducer.

(h) Heading--read from the aircraft's flux gate compass.

(i) Position--determined with a Teledyne 711 Loran C system. A Collins LRN-80 VLF/Omega long range navigation system is also used because Loran C signals, while more accurate than Omega, are frequently unreliable in the Greenland Sea region.

(j) Groundspeed--while it is measured directly by the Loran C and Omega systems, it has been found more accurate to compute it from the time required to go between known positions (as determined by the Loran or Omega systems).

(k) Mean winds--obtained from the difference between the airspeed and groundspeed. Making the runs upwind and downwind simplifies the computation by eliminating any crosswind component.

(l) Pressure altitude--measured with a pressure transducer.

(m) Radar altitude--measured with a Bonzair Mark 10 radar altimeter.

(n) Vertical electric field--measured with custom built electrometer systems which have been developed over the years. The signals are measured between two radioactive probe antennas (one on each wingtip).

(c) Electrical conductivity of air--measured with independent parallel plate Gerdien tubes. Each sign (+) and (-) is measured with a separate tube.

3. Determination of fluxes. Because we are able to measure the velocity structure function parameter G , it is possible to compute the heat, humidity and momentum fluxes. The dissipation method relies on semi-empirical relationships of inertial subrange turbulence to surface-layer scaling parameters. A discussion of how it is measured is given in Fairall et al (1980) while additional analysis and validation of the dissipation flux method is given by Fairall and Larsen (1984). Since the inertial subrange of locally isotropic turbulence is in the high frequency regime, the structure functions can be measured without correcting for platform motion. Thus these measurements can be made from a relatively small aircraft with simple equipment measuring scalars while the eddy correlation technique used on the larger aircraft requires gust probes and an inertial navigation system. A disadvantage of the dissipation method is that only the surface flux can be determined--the technique is not valid above the surface layer. However, it is the surface fluxes that are of interest to the MIZEX problems being investigated. Because the Baron aircraft can be routinely flown within a few meters of the ice/ocean surface, it can obtain data in the surface layer. A discussion of how the drag coefficient can be derived from these measurements is given by Garratt (1977).

The eddy dissipation technique for measuring fluxes has distinct advantages over the eddy correlation technique in an experiment such as MIZEX. It offers spacial resolution of 3 km (about 1 min of data averaging) compared to about an order-of-magnitude less spacial resolution with the eddy correlation technique because the latter requires statistical averaging of about 10-20 min of data per point (C.W. Fairall, 1983, personal communication; D. Lenchow, 1983, NCAR, personal communication). In addition, in the MIZ where we have measured very small fluxes (on the order of 10 W/m^2 or less) it would appear that the gust probe/INS instrumentation would not have the required sensitivity to measure such small fluxes.

4. Operational factors.

(a) Flight paths. The basic flight path chosen to study the PBL modification across the MIZ was upwind and downwind constant altitude runs from about 50-100 km on one side of the ice edge to a similar distance on the other side. The paths were arranged to cross the Polar Bjorn which was generally near the ice edge whenever possible (about 1/2 the time). The runs were generally made at a height of 13 m to match the location of the turbulence sensors on the ship's mast. This provided coherence between the aircraft and ship data as well as cross-calibrations when the aircraft flew past the ship. It was also found necessary to operate at such a low altitude in order to keep out of the low

stratus with ceilings frequently in the 30-50 m height range. Typically about 5 profiles were obtained on each horizontal run with one at each end of the line, one about 20 km on either side of the ice edge and one at the ship. When fog prevented the above relatively long runs, sometimes it was necessary to settle for one profile on each side of the ice edge. The vertical profiles extended from the sea surface up to 1.5 or 3.0 km, above the PBL in either case.

(b) Operating in fog

While flight could generally be conducted close to the surface over the ocean, it frequently was not possible to penetrate more than about 20 km over the ice because the thin foggy but non-cloudy area we were operating in disappeared as thicker fog formed or the stratus lowered to the surface. Visibilities in the clear area just above the ice/ocean were typically 1 to 2 miles down to 1/4 mile which was the minimum visibility required to maintain visual contact with the surface. When visibility became too low, the aircraft climbed through the stratus to above the PBL. The MIZEX test region was generally covered by low stratus clouds and in order to obtain the required meteorological data the aircraft flew to the test region in the clear at high altitudes and then as was necessary to penetrate the stratus down to the thin relatively clear area which was generally found just above the surface. This was possible through use of the radar altimeter and descents were made to a radar altitude of 150 feet. By this height it was usually possible to pick up the surface visually, if not, the aircraft climbed back up and tried again at another location. The air temperature at low altitude above the ice and ocean was always one to a few degrees above freezing so aircraft icing was not a problem.

(c) Navigation. Because the Loran C signals are unreliable in the Greenland Sea region, it was necessary to navigate by Omega and NDB (non-directional beacon) low frequency homing. Since the Omega drifts several miles per hour, the only way to locate the ships under the clouds was through their NDB beacons. When over a ship it was possible to benchmark the Omega navigation receiver with their position. It was found possible to use the ship's NDB beacon from a distance of 50 miles. The commercial radio station at Longyearbyen has a stronger signal which was useful out to about 150 miles.

5 Flights from Longyearbyen

During MIZEX-83 eleven flights were made in the test area operating from the airport at Longyearbyen, Spitsbergen. Table 1 summarizes these flights. Typical flight times were 6 to 7 hours with the photomosaic mission on 11 July taking 8.7 hours. The aircraft has a maximum duration of 10.5 hours. Except for a period when the aircraft was inoperative while awaiting a mechanical part (17-24 July), it was found possible to conduct flights and obtain

the desired data every day regardless of weather. This was because the Baron could be flown at low altitudes in fog and had the capability of landing back at Longyearbyen under conditions of minimal visibility.

6 Personnel

The personnel associated with the field program at Spitsbergen and their duties were:

--Dr. Ralph Markson (ARA), P. I., coordinator, pilot, instrumentation, aircraft maintenance.

--Mr. Hal Schnerr (ARA), airline transport rated pilot (1st part of field period)

--Lt. Cdr. Larry Conrad (ARA/U.S. Navy), airline transport rated and arctic pilot on leave from the Navy (2nd part of field period)

--Dr. Chris Fairall (Penn State), aircraft observer, instrumentation, data reduction and analysis.

--Mr. George Lockwood (Penn State graduate student), aircraft observer, data reduction.

--Dr. Ed Zeller (University of Kansas), antarctic researcher, in charge of photography, aircraft maintenance and general project support.

--Mr. James Busse (University of Kansas), professional photographer, Hasselblad camera operator, operation of darkroom set up at Longyearbyen, assembly of mosaic and transect photography.

--Dr. Gisela Dreschhoff (University of Kansas), antarctic researcher, assembly of photomosaic, general project support.

7. Examples from preliminary data analysis

Analysis of the entire data set acquired by the Baron during MIZEX-83 is an appreciable task which will be conducted by C. W. Fairall at Penn State under a separate ONR contract. Some interesting examples of the flux variations from preliminary analysis of the flights made on 15 July 83 and 30 July 83 will be discussed next.

The surface heat flux and stress for the two flights showed considerable horizontal variation from the ocean to pack ice (Figs. 1a and b). On 15 July (Fig. 1a) the surface wind was roughly parallel to the ice edge at 5 m/s. The stress was about 50% higher over the ice and MIZ. The strong peak in stress and heat flux at -25 nm is due to an Arctic lead approximately 10 miles in width (parallel to the ice edge). The lead also shows up as a small bump

in the surface temperature. On 30 July (Fig. 1b) the surface wind was off-ice at 4.5 m/s (5 m/s over the ice and 4 m/s over the ocean). Heavy fog over the pack ice invalidated the turbulence data (due to droplet impact on the sensors) so the surface flux data stops at -15 nm.

Typical meteorological flights produced about 6 spiral profiles. Three examples that illustrate some interesting boundary layer effects have been chosen (Figs. 2a, b and c). The locations of the profiles are indicated in Fig. 3. On 25 July (Fig. 2a) the wind was parallel to the ice edge (220 degrees at 2.5 m/s). The PBL depth over the ocean is about 500 m with a stratocumulus deck from 100 to 500 m. Note on the 25-1 profile a hint of a stable surface layer is present in the lowest 50 m of the θ_v profile. Despite the strongly stable surface layer over the ice (25-2 in Fig. 2a) a well-mixed boundary layer is maintained up to 500 m by cloudtop radiative cooling production of turbulent kinetic energy. The 6 degree boundary layer temperature difference indicates a 5 m/s baroclinic wind component from the north.

On 27 July (Fig. 2b) the wind was southerly but slightly on-ice (160 degrees at 6 m/s). PBL stratocumulus clouds were present over the ocean with tops at 650 m and bases at 250 m (27-1 in Fig. 2b). Over the ice the PBL depth was only 300 m leading to a baroclinic wind component from the south of about 7 m/s (primarily due to the sloping inversion).

On 28 July (Fig. 2c) the wind was on-ice (130 degrees at 6 m/s). Over the ocean a well-mixed boundary layer was completely filled with PBL stratocumulus from 800 m (top) to 30 m (base). The vertical gradient in θ_v is a wet adiabat and the vertical gradient in q is due to conversion of vapor to liquid water and indicates a linear liquid water profile in the cloud. A stable surface layer quickly formed over the ice (28-2 in Fig. 2c).

Although our analysis of MIXEX-83 data is not complete, a few initial observations are summarized in Table 2.

C. Photography.

The Baron was equipped for aerial photography with a downward pointing Hasselblad camera looking through an optical glass window in the belly of the fuselage. The camera was a model 500EL using a 40 mm lens. For the mosaic the camera was controlled by an intervalometer adjusted for about a 30% overlap between frames. J. Busse flew as camera operator and deserves credit for this fine product. He assembled approximately 300 pictures into the final mosaic after enlarging and rectifying individual pictures to match each other. All the Hasselblad imagery was taken during the filming of the mosaic which was made from 10,500 ft. The film was Kodak Plus-X Aerographic 2402 (70 mm). The mosaic was made over a 4-hour period near midnight on 11 July. It covers the region imaged several hours earlier by the ERIM SAR radar and the NFL

passive microwave system

A darkroom was set up at the Norsk Polar Institute where the film was processed and printed so that individual pictures from the mosaic were available the day after they were taken and the first copy of the mosaic was finished about a week after it was photographed. The resolution of the imagery was 1-2 m as determined by photographs of the Polar Stern in the mosaic. By photographing the same region of an ice field at two different times, it was found that the relative motions of the ice could be determined; an example of this will be shown (Picture 2)

Besides the mosaic, a 35 mm Olympus camera was used for hand held oblique photography from the cabin windows and for downward looking transects through the optical window. Two transects were obtained on 29 July from the ice edge about 30 km south of the Polar Stern (where helicopter-borne personnel were studying the ice) toward the ship. One of these transects crossed over the ship and ended a few km beyond it. These were made with color transparency film (slides).

Additional 35 mm color transect photography was obtained along a scalloped ice edge on 31 July specifically to document this phenomenon for E. Mollo-Christensen. An array of streaks on the water next to the scalloped ice edge was also photographed and meteorological profiles were obtained on both sides of the ice edge.

Appendix B contains (a) a copy of the mosaic, (b) an example of ice motions derived from two temporally spaced photographs and (c) some interesting features in individual pictures from the mosaic.

D. Availability of Data.

The meteorological data are being archived by R. Markson at Airborne Research Associates and C. W. Fairall in the Department of Meteorology at the Pennsylvania State University. These data consist of the set of vertical profiles (contained here in Appendix A) and tables listing 15-sec average values of the following parameters measured during low altitude horizontal runs.

- position
- time
- pressure
- altitude
- air temp
- dew pt temp
- sea surface temp
- water vapor density
- virtual potential temp
- relative humidity
- velocity structure function no. 1

--velocity structure function no.2 (redundant)
--temperature structure function
--humidity structure function

This data is not included here as it comprises some 305 pages

The photography consists of the black and white mosaic which was hand made by James Busse, Rt 1, Box 176-S, Perry, Kansas 66073 (913)597-5509. A copy of this has been given to the Environmental Research Institute of Michigan and additional copies will be distributed to the laboratories that participated in MIZEX-83 in the near future when they are available. Additional copies can be obtained from Mr. Busse for a nominal reproduction cost. Sizes up to 16"x20" can be made from the master relatively easily. Blowups of individual frames (which can be identified from the "preliminary index mosaic") can be provided by Mr. Busse.

In addition, ARA obtained 35 mm color transects taken from about 200m altitude. These consist of single lines of overlapping pictures lasting for a single roll of film (36 pictures). Two such transects were obtained on 29 July from the ice edge south of the Polar Bjorn toward the ship which was at 77-00N, 02-55W. Another transect was obtained on 31 July along a scalloped ice edge near 76-06N 02-00W. This will be provided to E. Mollo-Christensen.

There were also numerous hand held 35 mm color slide images made of interesting features of the ice field and shots of the Polar Bjorn. Copies of the 35 mm photography will be provided for specific requests sent to R. Markson at ARA.

E References.

Fairall, C.W., R. Markson, G.E. Schacher and K.L. Davidson, 1980: An aircraft study of turbulence dissipation rate and temperature structure function in the unstable marine atmospheric boundary layer, Boundary-Layer Meteorol., 19, 453-469.

Fairall, C.W. and S.E. Larsen, 1984: Inertial-dissipation methods and turbulent fluxes at the air-ocean interface (in preparation).

Garratt, J.R., 1977: Review of drag coefficients over oceans and continents, Mon. Weath. Rev., 105, 915-929.

Table I. SUMMARY OF MIXEX-83 FLIGHTS BY ARA BARON

<u>Date</u>	<u>Flt. No.</u>	<u>Length Flt.</u>	<u>Ship Pos.</u>	<u>Comments</u>
11 July	1	8.7 HRS	79°39'N 02°41'E	Ship is Polarstern. Obtained unbroken mosaic of about 350 pictures in desired region within hours after SAR image by CV-580, region approximately 79°23' to 79°49'N between 1°30' and 3°30'E. Photo resolution approaching 1 meter. The mosaic was obtained from 10,500 ft. under cloudfree conditions (which was quite rare).
14 July	2	3.9	79°21'N 1°32'E	From here ship is Polarbjorn. Met SNDGS and horiz turb/stress measurements from ocean to across ice. Met ship. Good data.
15 July	3	5.9	79°12'N 2°36'E	Stress runs at 50', 100' across MIZ, soundings. Met ship. Good data.
16 July	4	1.5		One sounding off coast of Spitsbergen. Returned to Longyear (partial power 1 engine) after exhaust manifold broke.
25 July	5	6.6	79°10'N 3°03'E	Two low level met runs past ship across MIZ. Good data. Aircraft repaired with parts sent from U.S.
26 July	6	4.2	79°00'N 1°49'E	Tried to photograph north box near 81°N for Campbell after ship reported "clear skies", and so did satellite. When we got there found solid clouds over entire MIZ test region. Did sounding from SFC to 28,000 ft. enroute.

Table I. SUMMARY OF MIXEX-83 FLIGHTS BY ARA BARON (CONTINUED)

<u>Date</u>	<u>Flt. No.</u>	<u>Length Flt.</u>	<u>Ship Pos.</u>	<u>Comments</u>
27 July	7	6.2	78°37'N 1°49'E	Calibration of aircraft met instruments next to ship. Low level met runs and soundings across MIZ. Good data.
28 July	8	5.7	77°57'N 3°50'W	Further cross calibration (ship/aircraft), developed mean wind measuring technique using LORAN. Horizontal and vertical met soundings. Bulk met data O.K. but turb. data probably no good (broken probes).
29 July	9	7.1	77°00'N 5°55'W	Calibration at ship, including ladder turbulence profiles. Horizontal low level runs past ship across MIZ. Ice transect photography at ice edge 18 mi. S. of ship at their request. Mean wind comparison with ship indicates agreement within 2 kts. Good data.
30 July	10	7.2	75°43'N 1°40'W	Most complete met data so far due to less cloudiness. Five soundings from ship to ice edge 60 mi. N.W. and continuing to 65 mi. into ice. Also 50' and 100' stress runs along this line. Good data.
31 July	11	7.4		Two sets of vertical soundings 20 mi. each side of ice edge. Photograph strip along ice edge including Mollo-Christensens' scalloped ice edge. Good data.

Table II.

Observations from MIZEX-83

Surface Properties

Preliminary examination of low-level runs from two flights (#3, #10) yielded the following information:

1. Stress was about a factor of two higher over the ice
2. Total heat flux was about 30 w/m² over the ocean and near zero over the ice.
3. The low level winds were roughly the same from ocean to pack ice.
4. The surface layer was stable over the ice.
5. The surface layer could be stable or unstable over the ocean.
6. Stability effects on the drag coefficient were substantial.

Boundary Layer Observations

1. Fog was common over ice.
2. Low level stratocumulus was common over the ocean.
3. Off-ice winds gave stable to convective PBL transitions; on-ice winds gave vice versa.
4. Stable PBL were about 100m deep.
5. Baroclinic effects were substantial.

Other Observations

Clouds above the PBL were often quite different over the ice than over the ocean. This implies mesoscale convergence effects to considerable altitudes (1.5 km).

MIZEX-83
 07/15/83 20:04Z
 +79 39'00'' N
 +003 51'00'' W

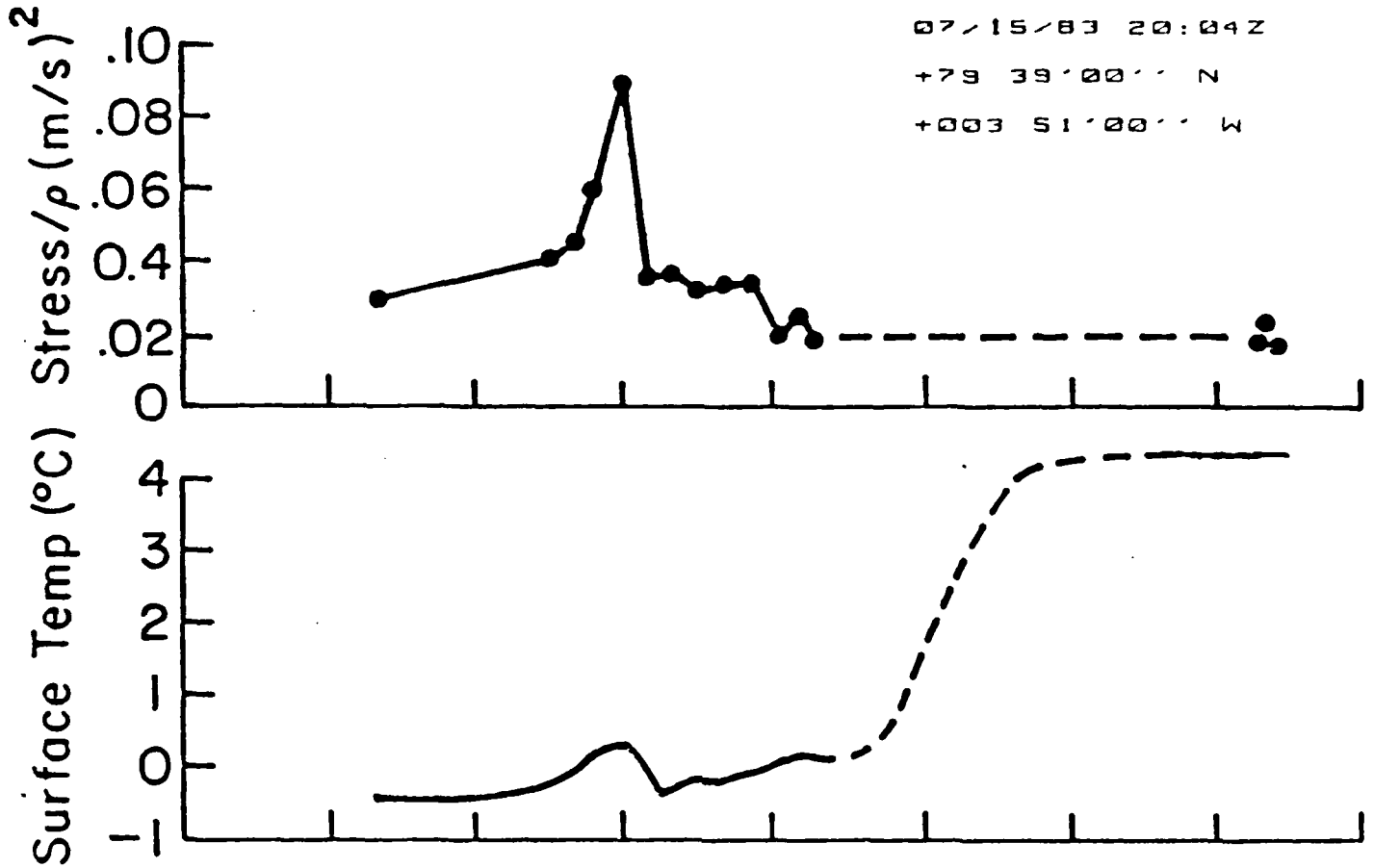
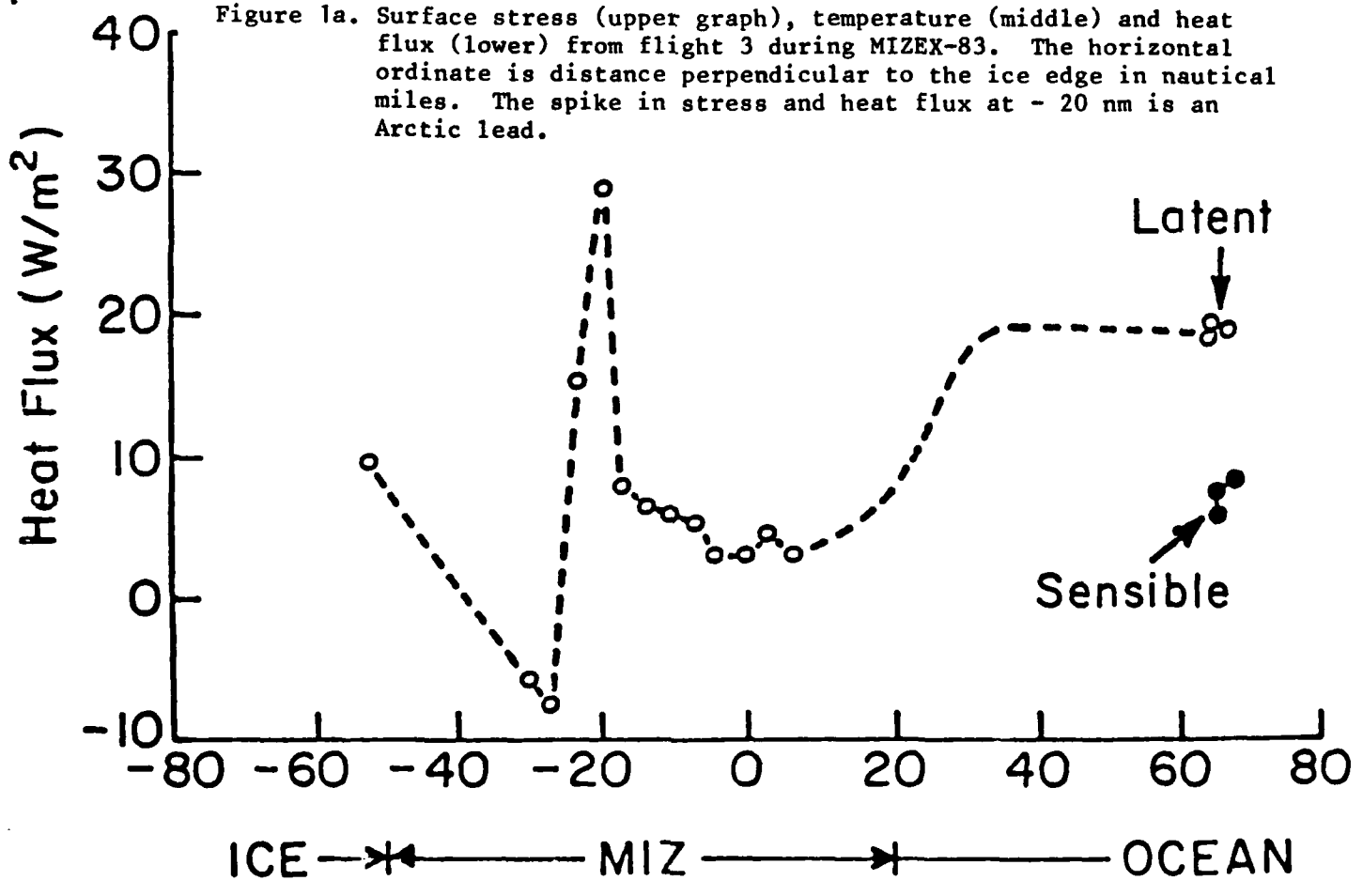


Figure 1a. Surface stress (upper graph), temperature (middle) and heat flux (lower) from flight 3 during MIZEX-83. The horizontal ordinate is distance perpendicular to the ice edge in nautical miles. The spike in stress and heat flux at - 20 nm is an Arctic lead.



MIZEX-83
07/30/83 15:46Z
+76 18'55'' N
+033 40'46'' W

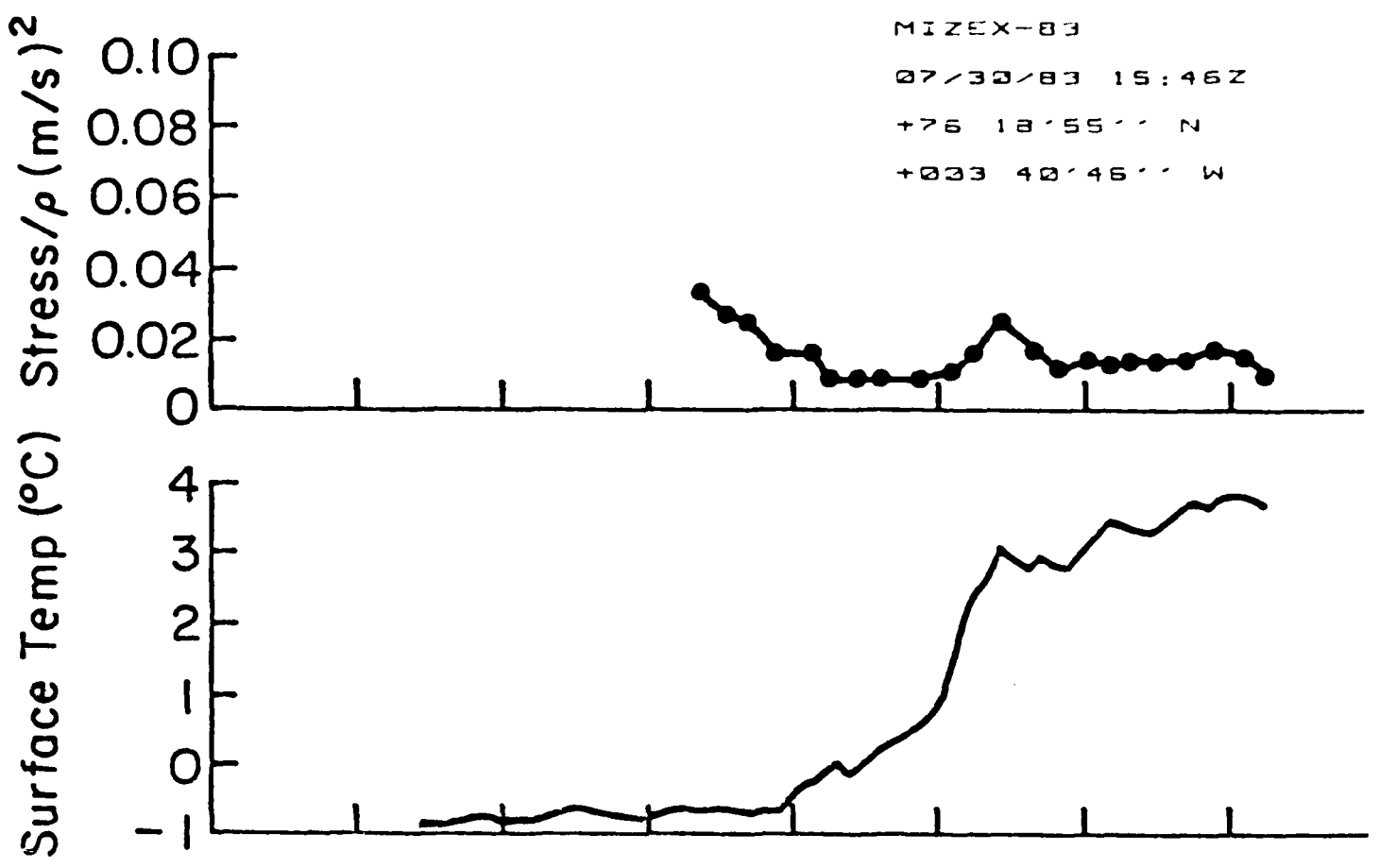


Figure 1b. Similar to Fig. 1a but for flight 10.

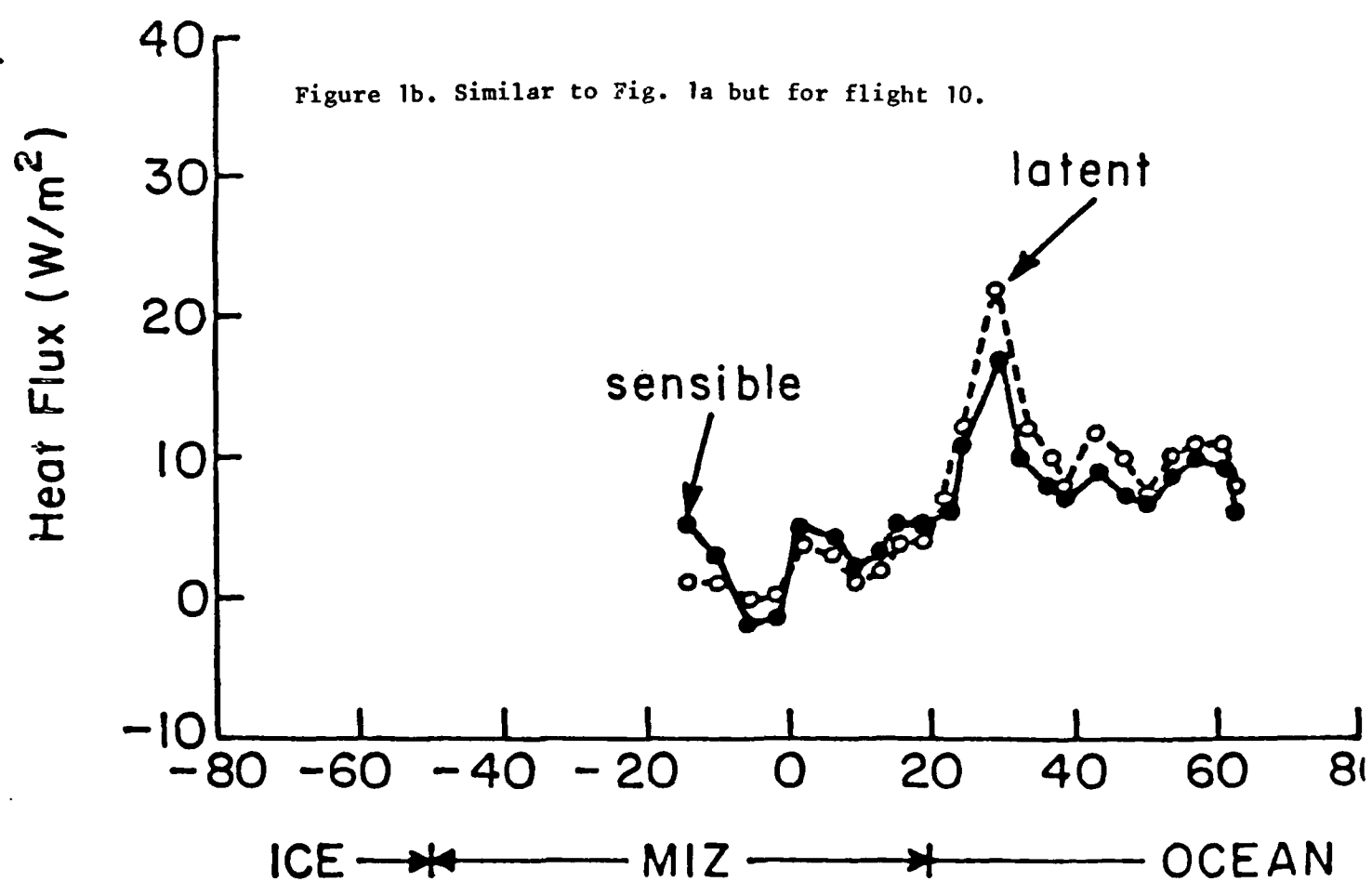


Figure 2a. Virtual potential temperature, θ_v , (solid line) and specific humidity, q , (dashed line versus altitude from MIZEX-83).

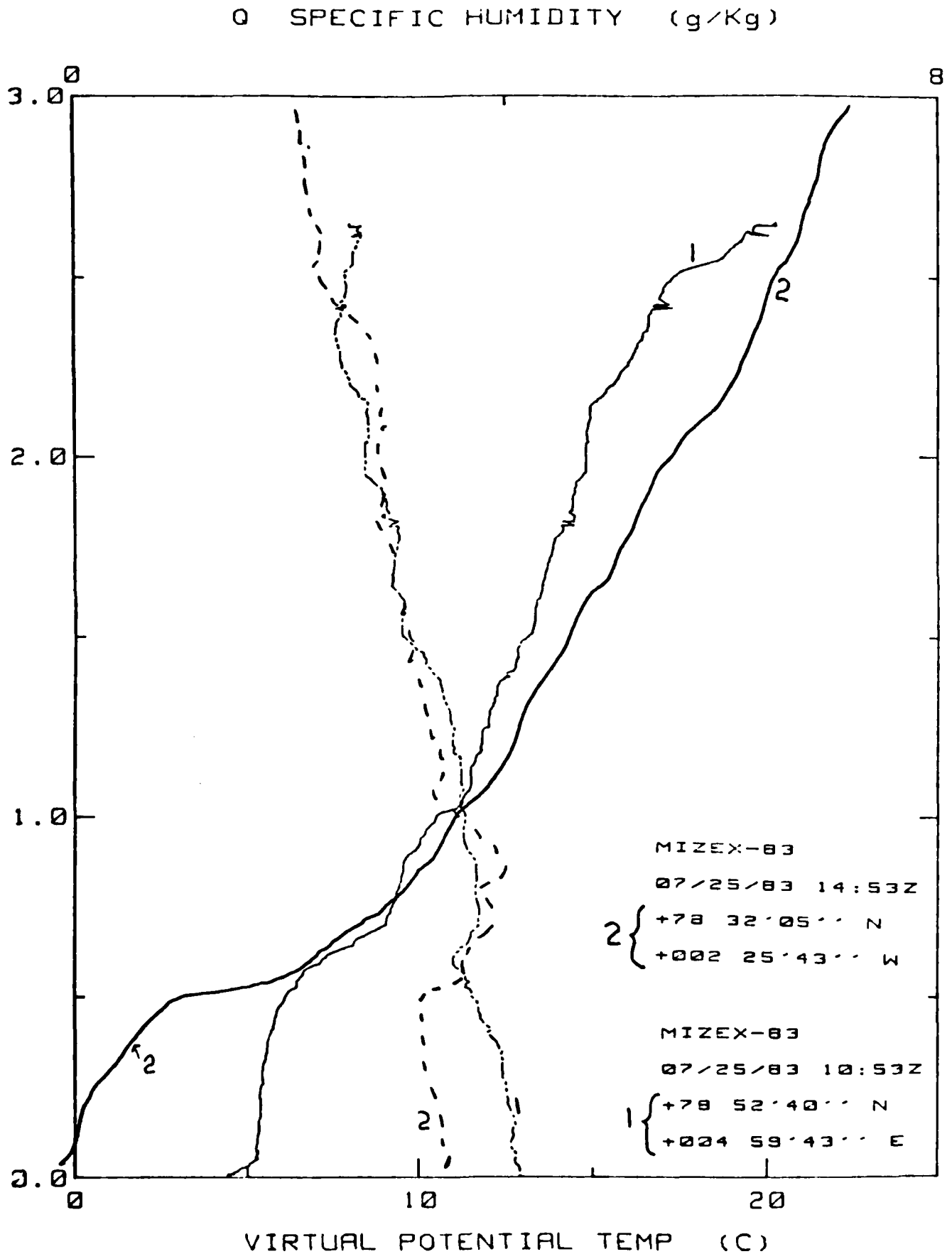


Figure 2b. Similar to Fig. 2a but for flight 7.

Q SPECIFIC HUMIDITY (g/Kg)

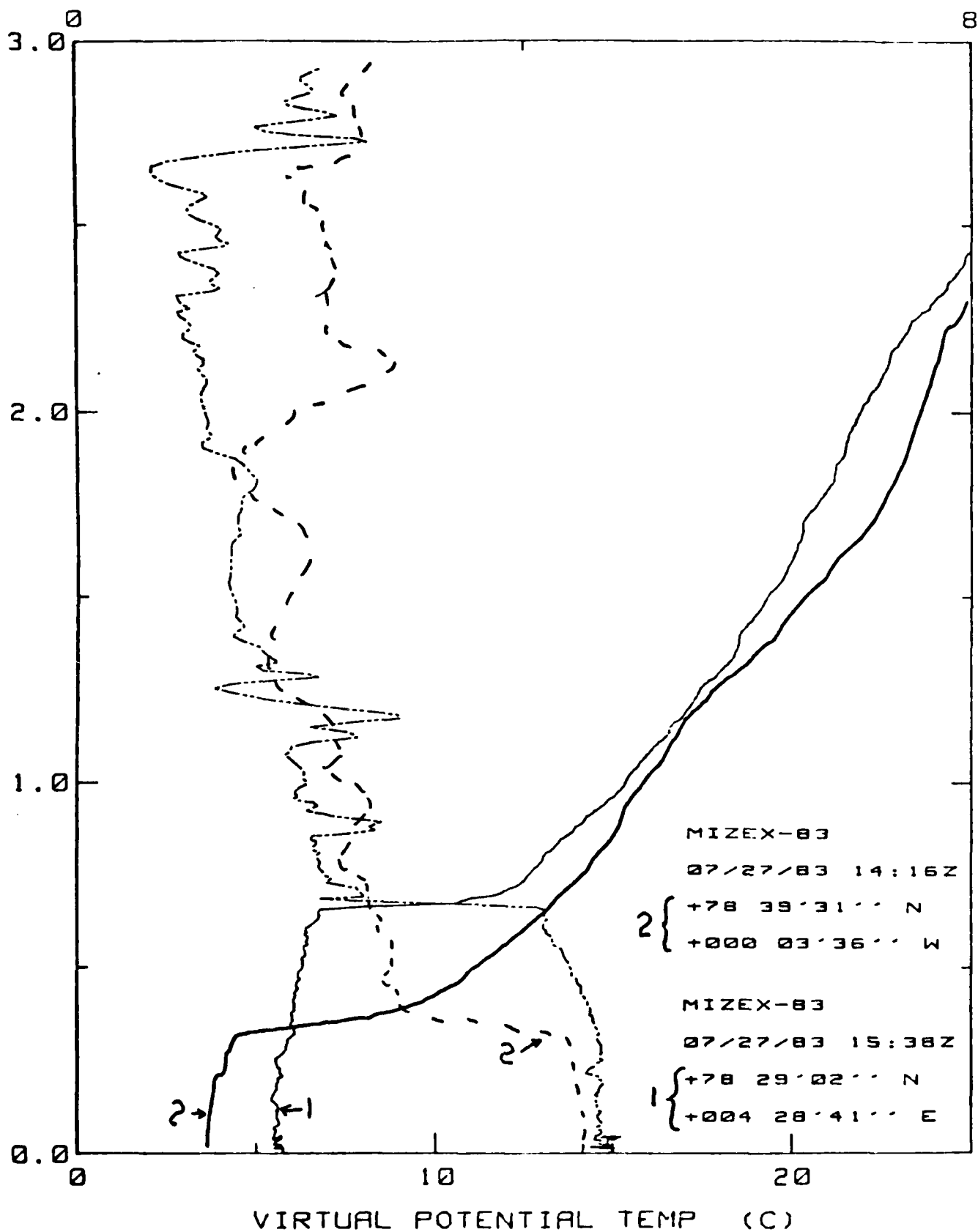
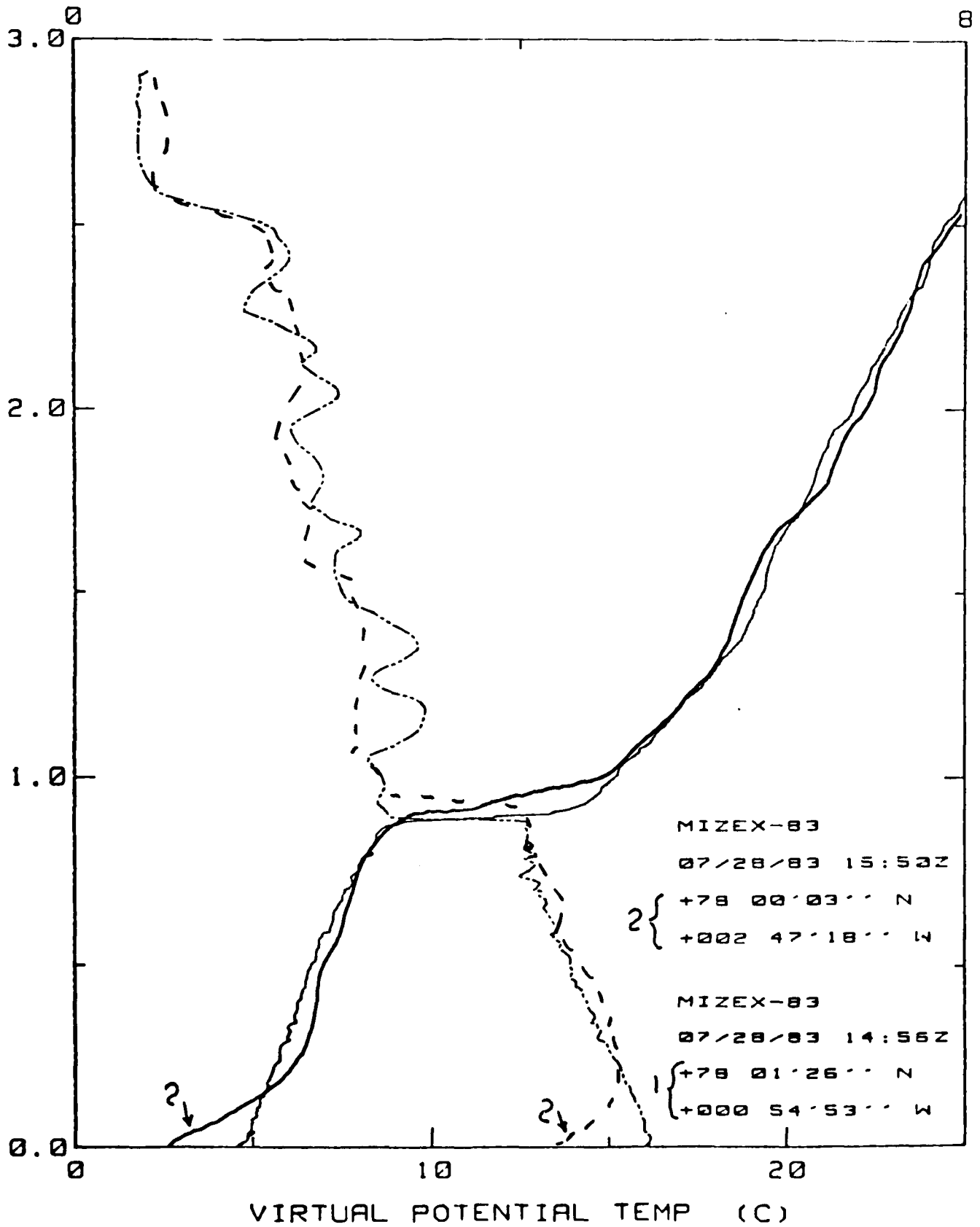


Figure 2c. Similar to Fig. 2a but for flight 8.

Q SPECIFIC HUMIDITY (g/Kg)



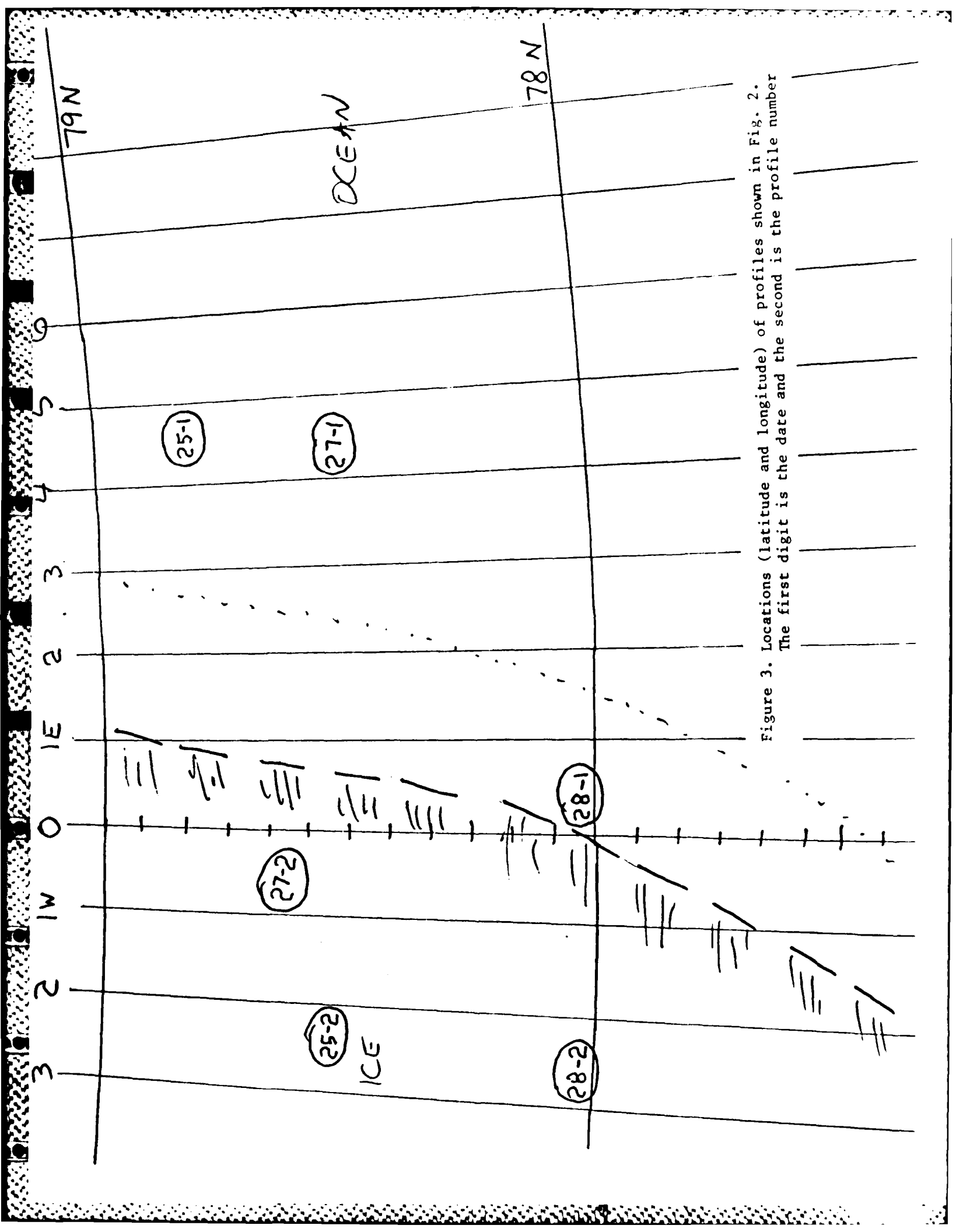
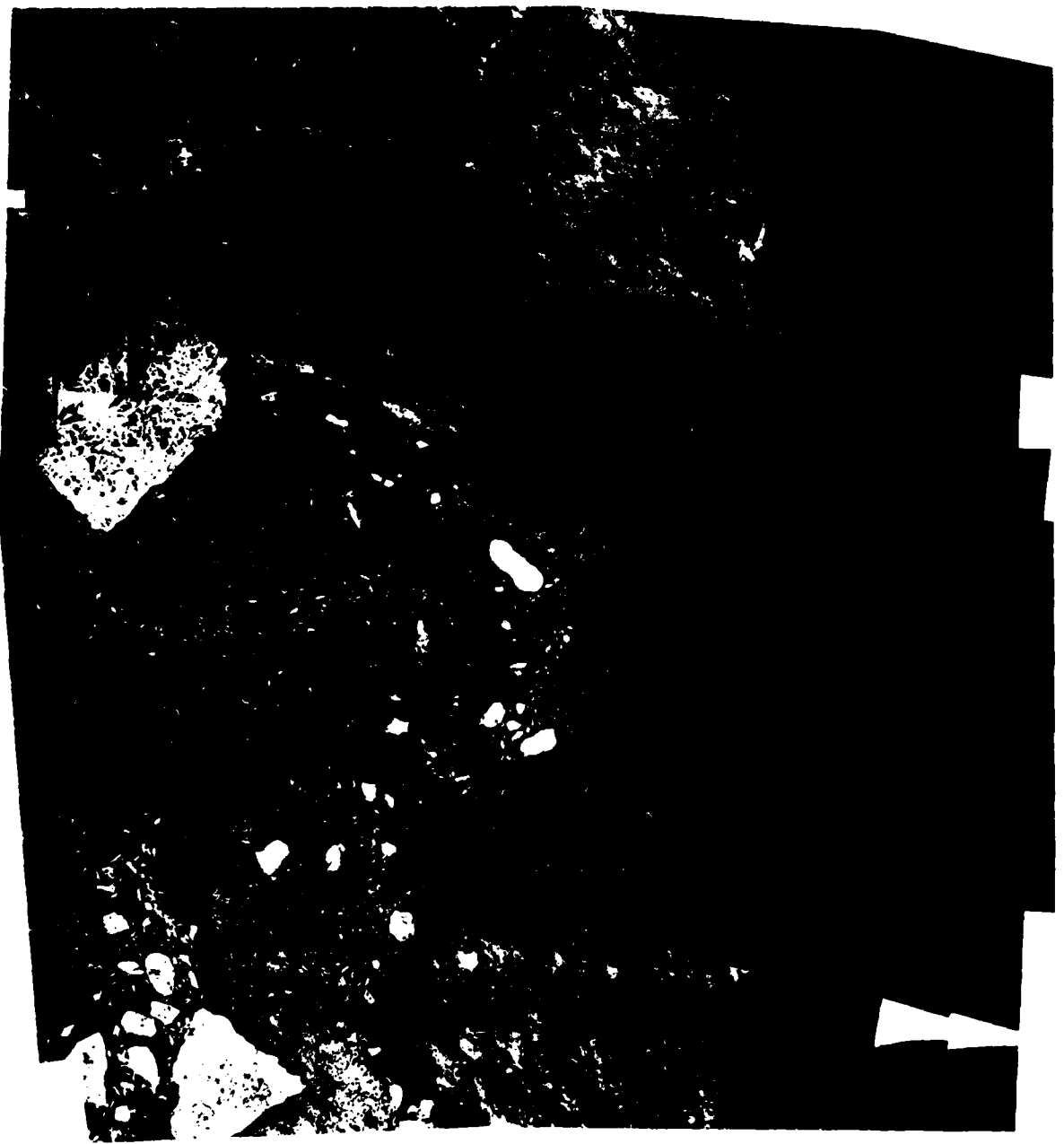
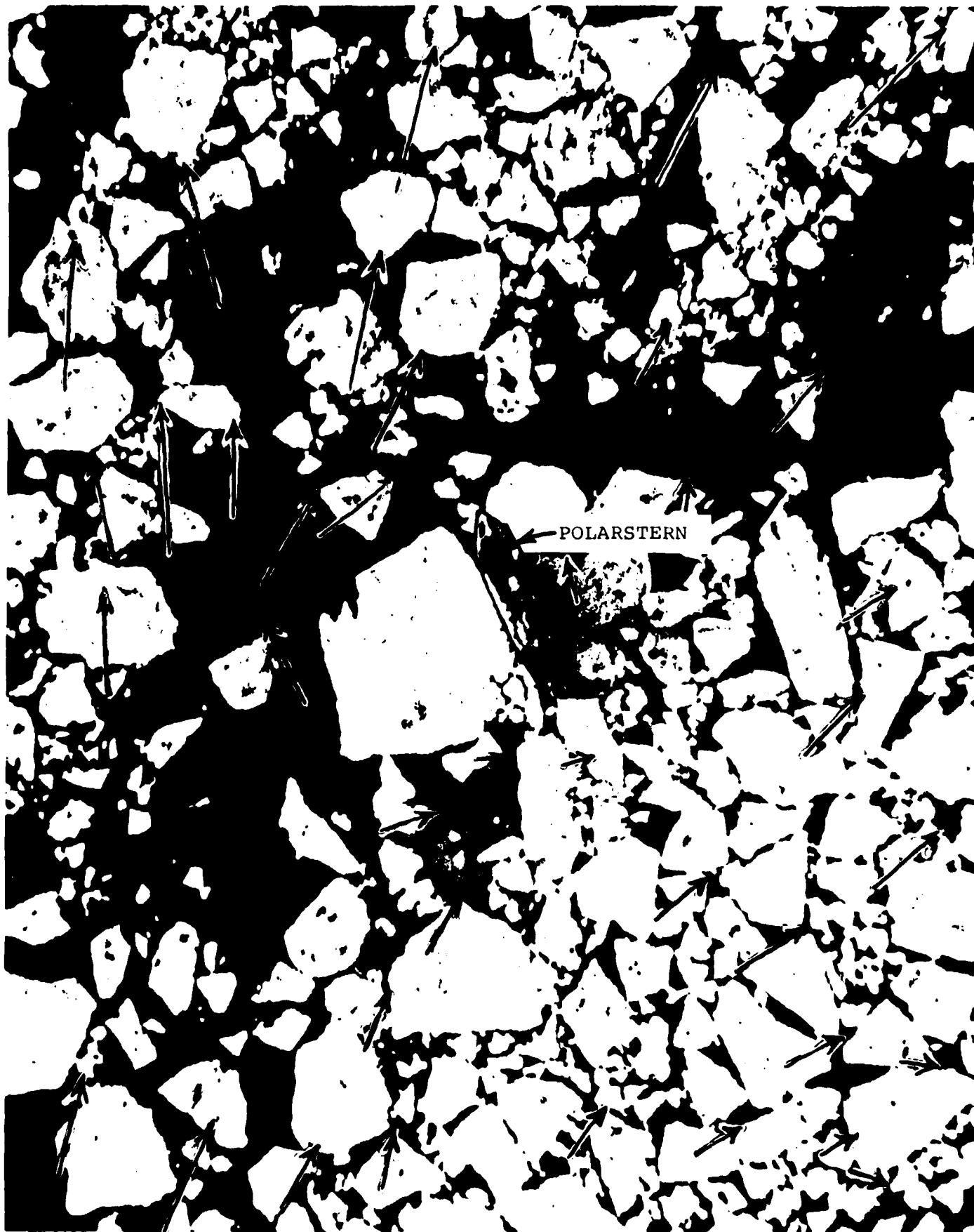


Figure 3. Locations (latitude and longitude) of profiles shown in Fig. 2. The first digit is the date and the second is the profile number

Picture 1. Mosaic obtained between 2148 UT, 11 July and 0141, 12 July 1983 of the region bounded by 79-23N to 79-49N; 01-30E to 03-30E. North is at the top. The aircraft flew E-W transects starting at the bottom of the box. The Polar Stern (at the tip of the pointer) was at 79-39N; 02-41E. Approximately 300 pictures were assembled into this mosaic. Enlargement of the picture containing the ship (Picture 2) gives a 1 to 2 meter resolution.

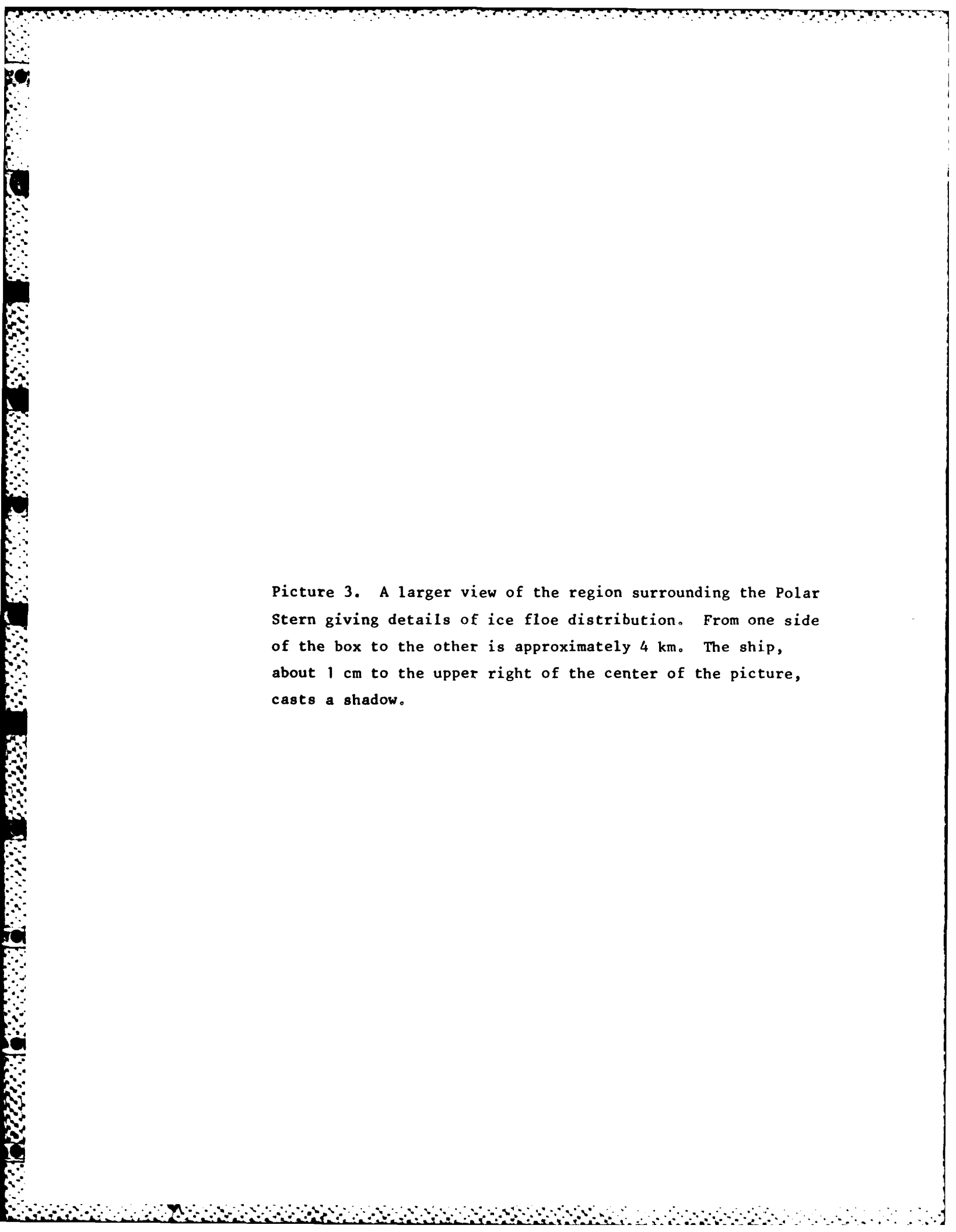


Picture 2. Enlargement of one frame of the mosaic containing the Polar Stern. A second picture of this area was obtained 8 minutes later during the next transect. Relative ice motions (movement of points in the ice field) during this interval are indicated by arrows. These movements were inferred by assuming the large square ice floe the ship is next to did not move. Since the ship is 150 meters long, it is calculated that the square floe about 3 cm above the ship was moving toward the upper right at about 0.3 knots.

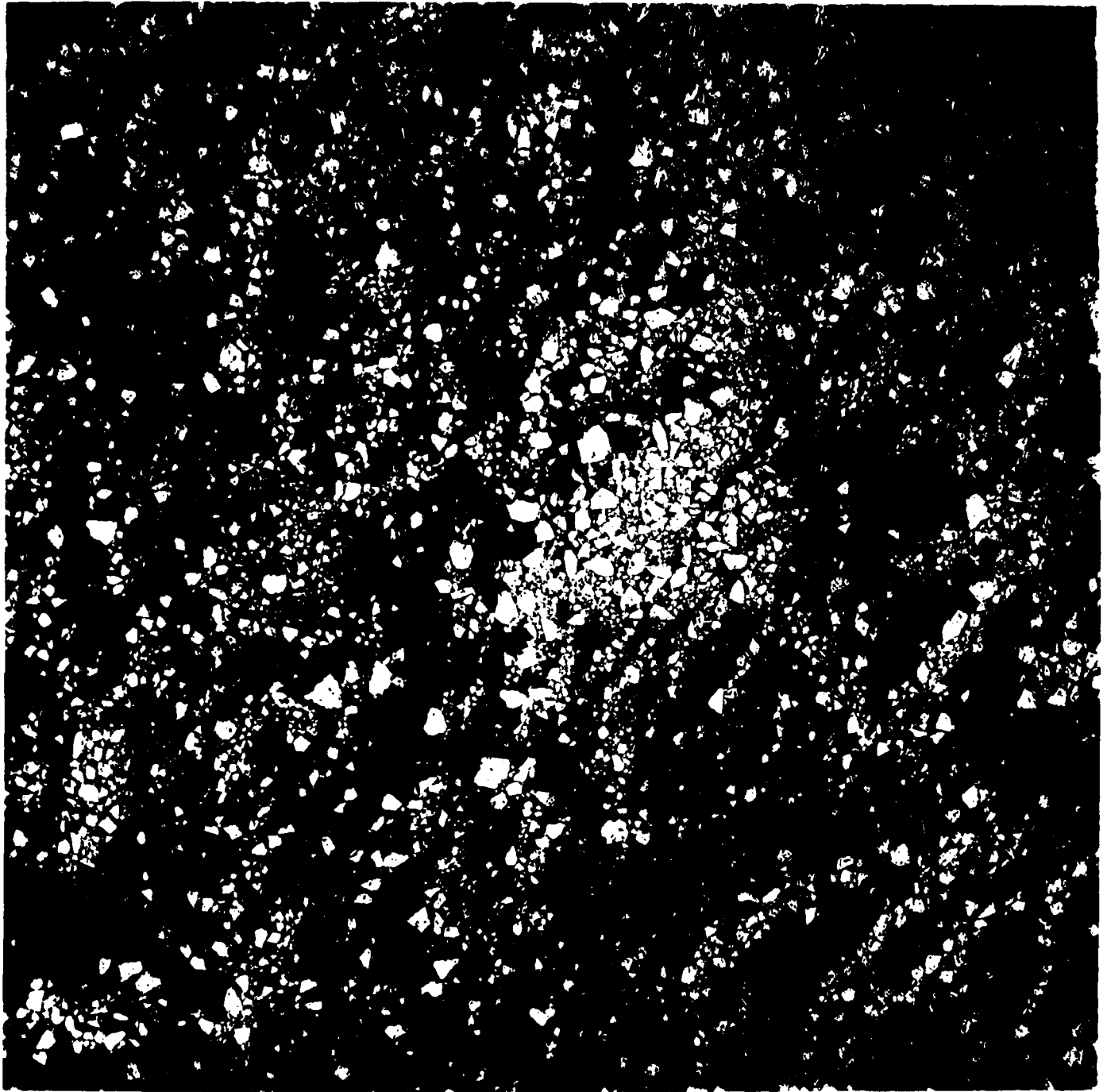


POLAR STERN Line 17, Frame 10 Scale - 1:2,800

RELATIVE ICE MOTIONS DETERMINED FROM TWO PHOTOS 8 MIN APART (11 Jy 83)

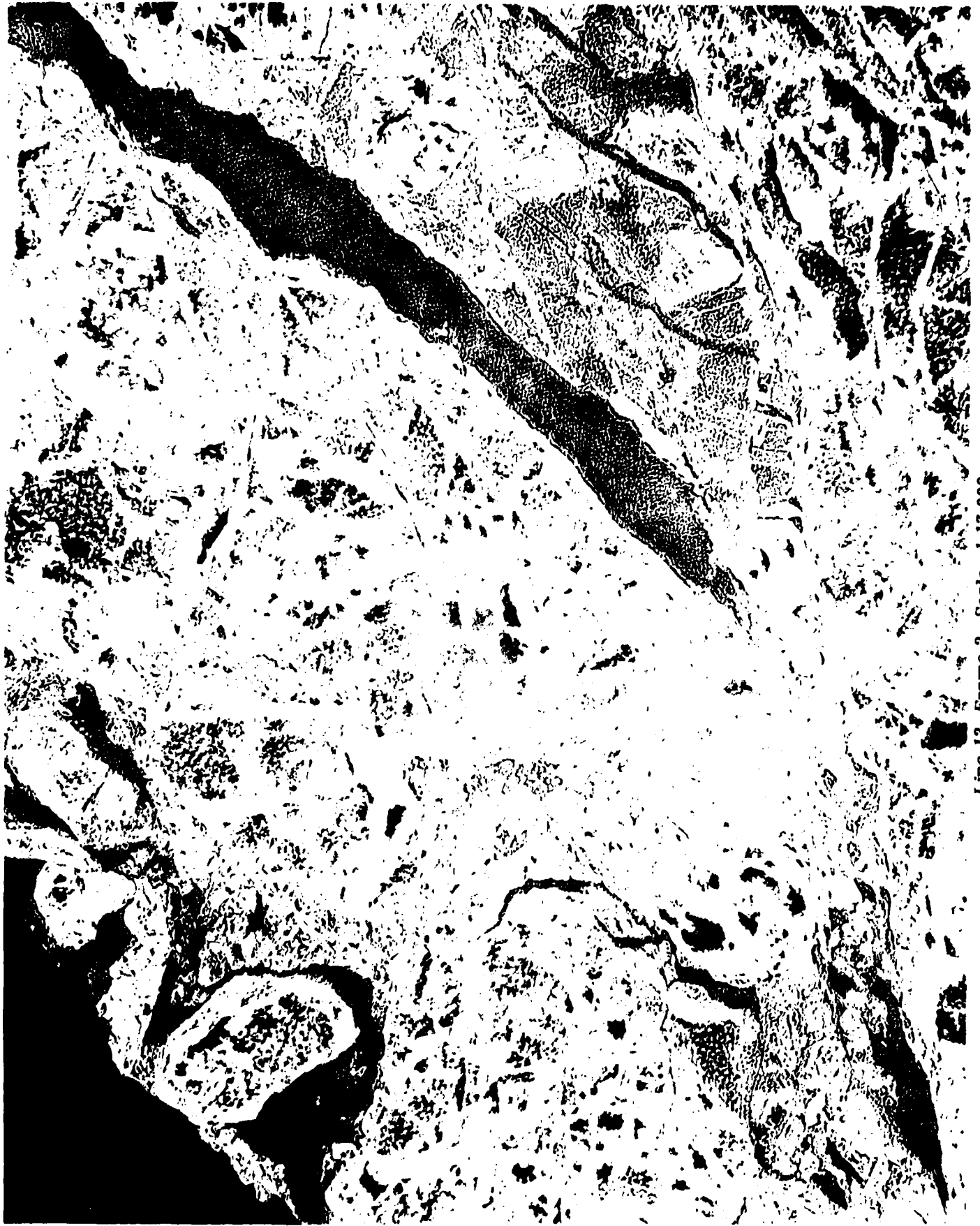


Picture 3. A larger view of the region surrounding the Polar Stern giving details of ice floe distribution. From one side of the box to the other is approximately 4 km. The ship, about 1 cm to the upper right of the center of the picture, casts a shadow.



POLAR STERN Line 17, Frame 10 Scale - 1:21,000

Picture 4. Structural details in the large ice island
in the upper left of the mosaic.



Line 13, Frame 2 Scale - 1:17,000

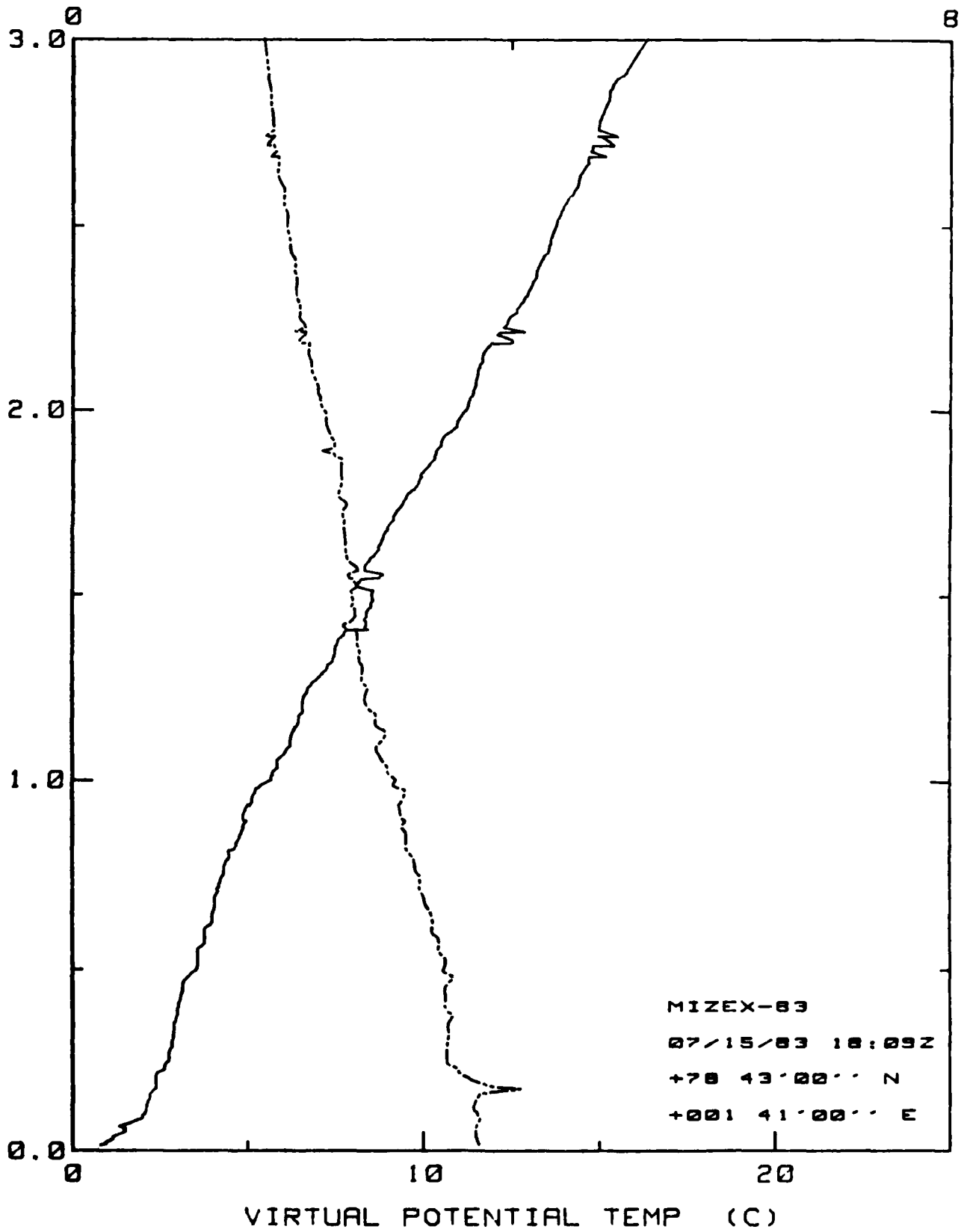
Picture 5. Details of two prominent ice floes near the center of the lower left quadrant of the mosaic. The larger floe is approximately 1 km wide.



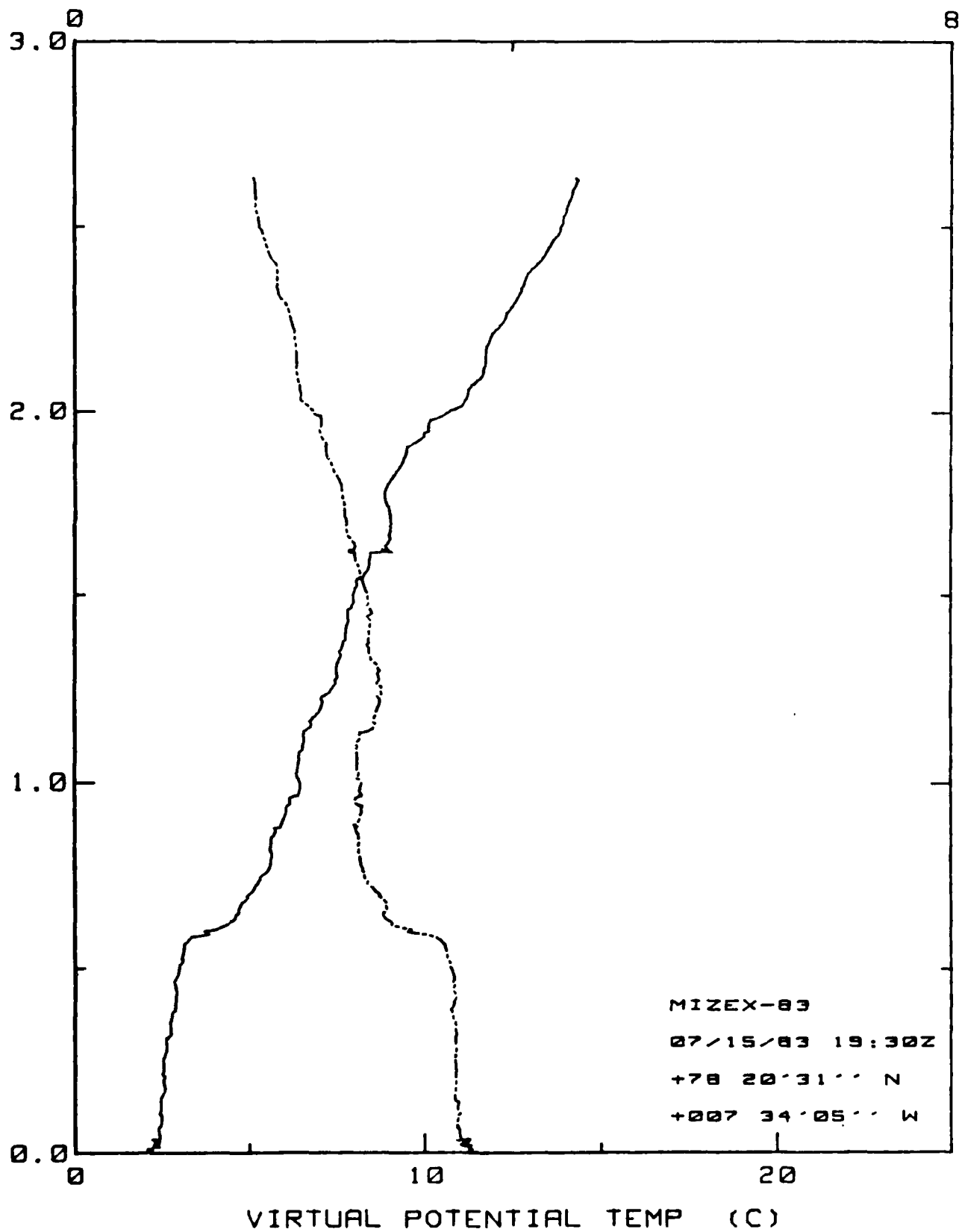
Line 5 Frame 6 Scale - 1:17,700

APPENDIX A

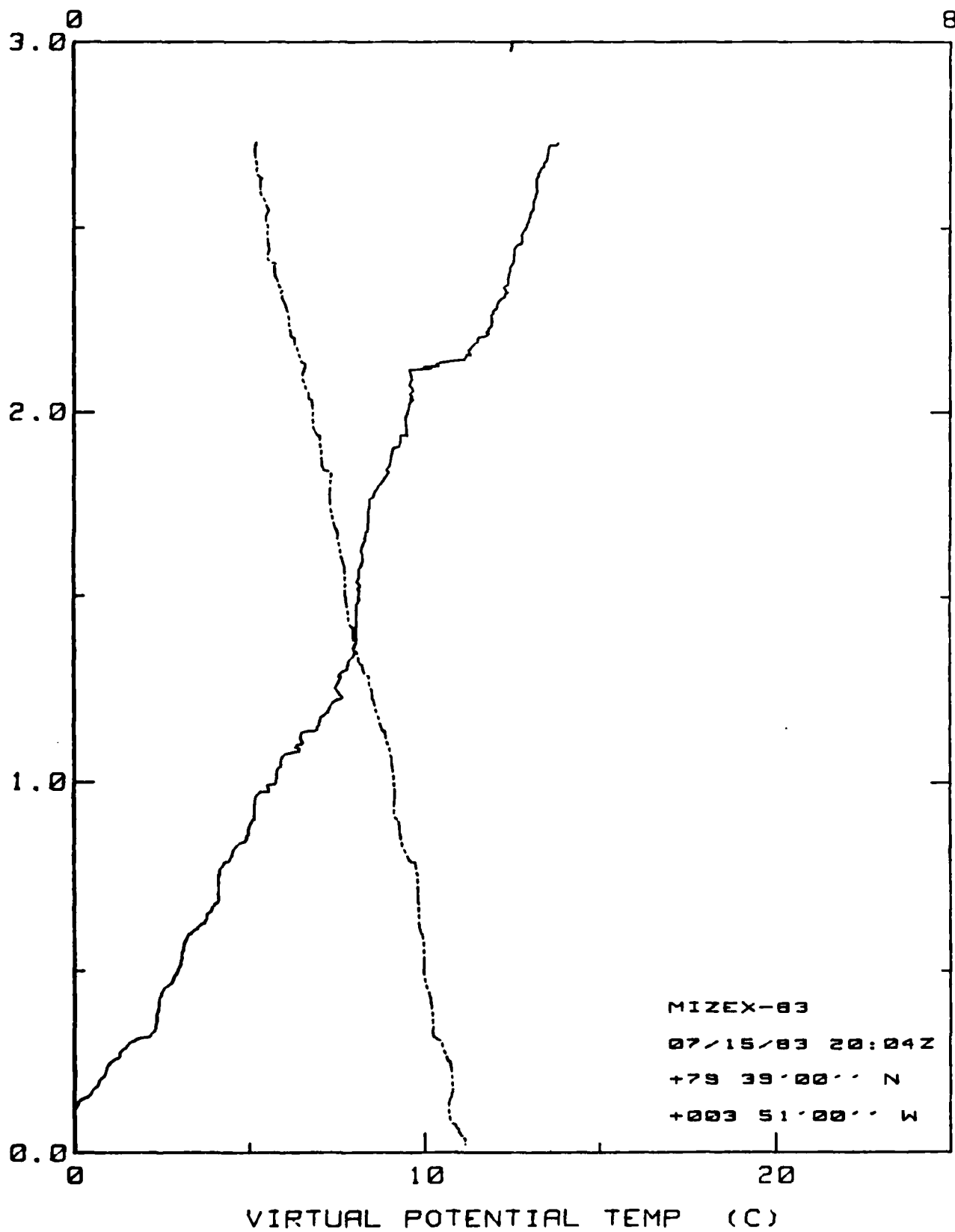
Q SPECIFIC HUMIDITY (g/Kg)



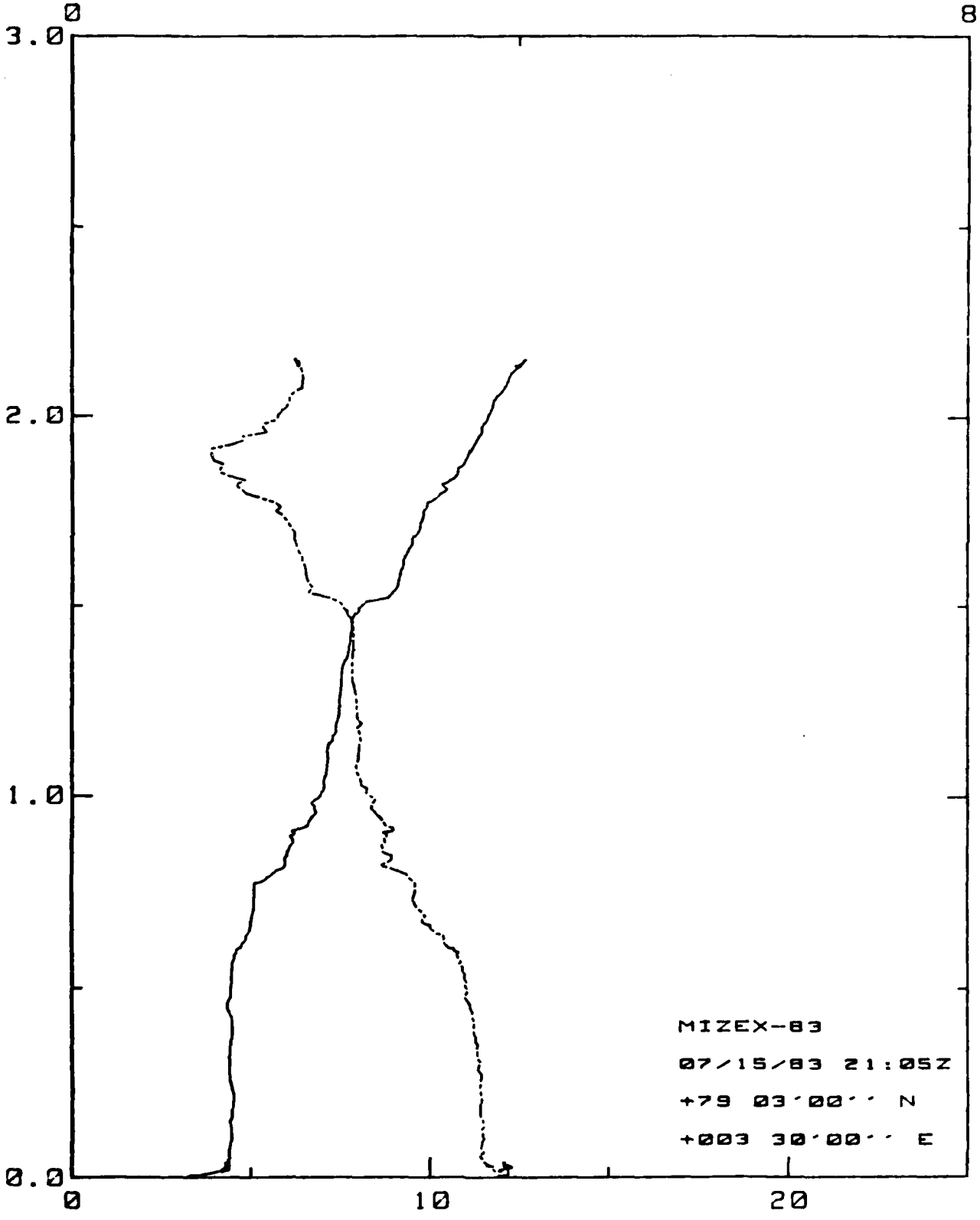
Q SPECIFIC HUMIDITY (g/Kg)



Q SPECIFIC HUMIDITY (g/Kg)



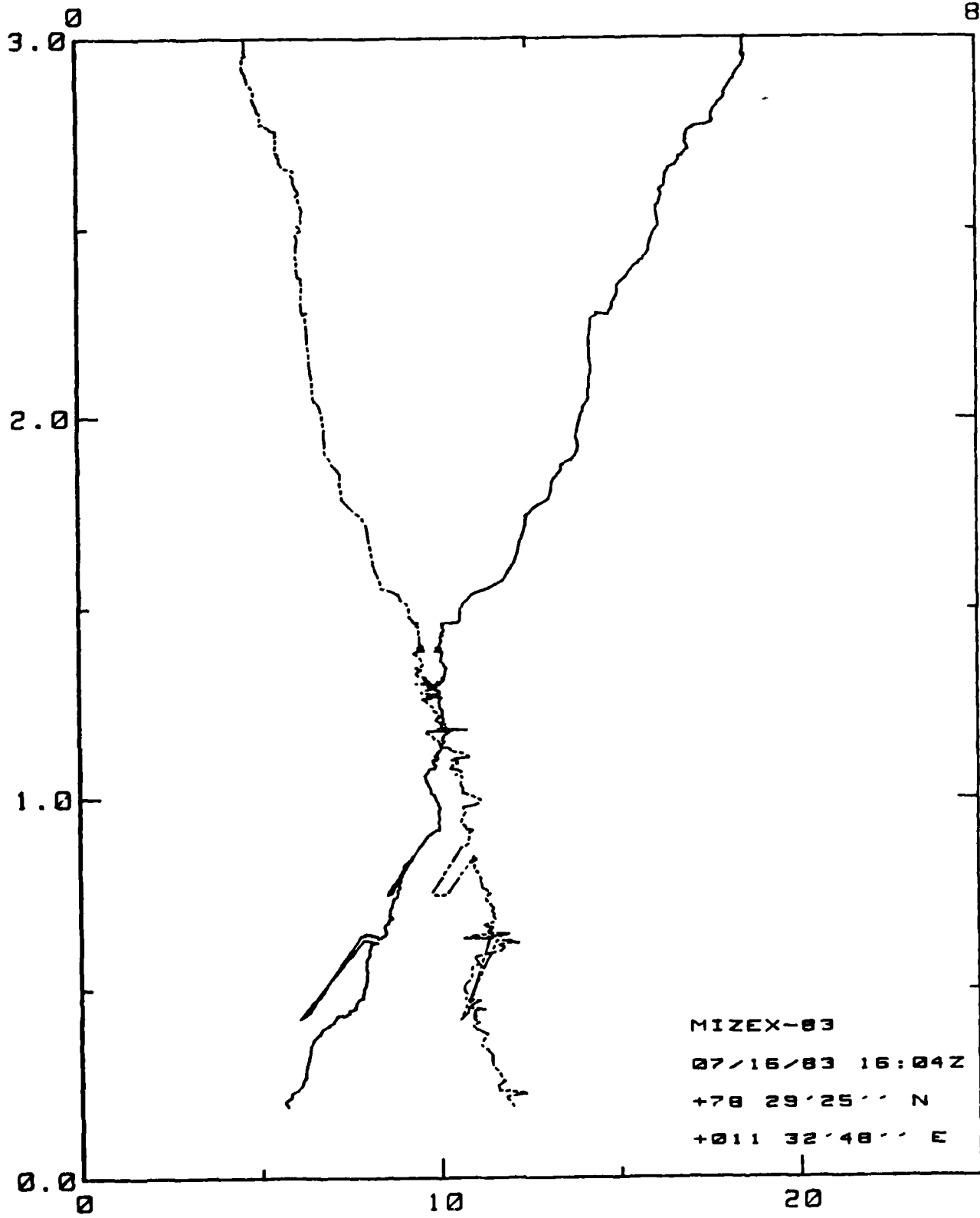
Q SPECIFIC HUMIDITY (g/Kg)



MIZEX-83
07/15/83 21:05Z
+79 03'00'' N
+003 30'00'' E

VIRTUAL POTENTIAL TEMP (C)

Q SPECIFIC HUMIDITY (g/Kg)



MIZEX-83

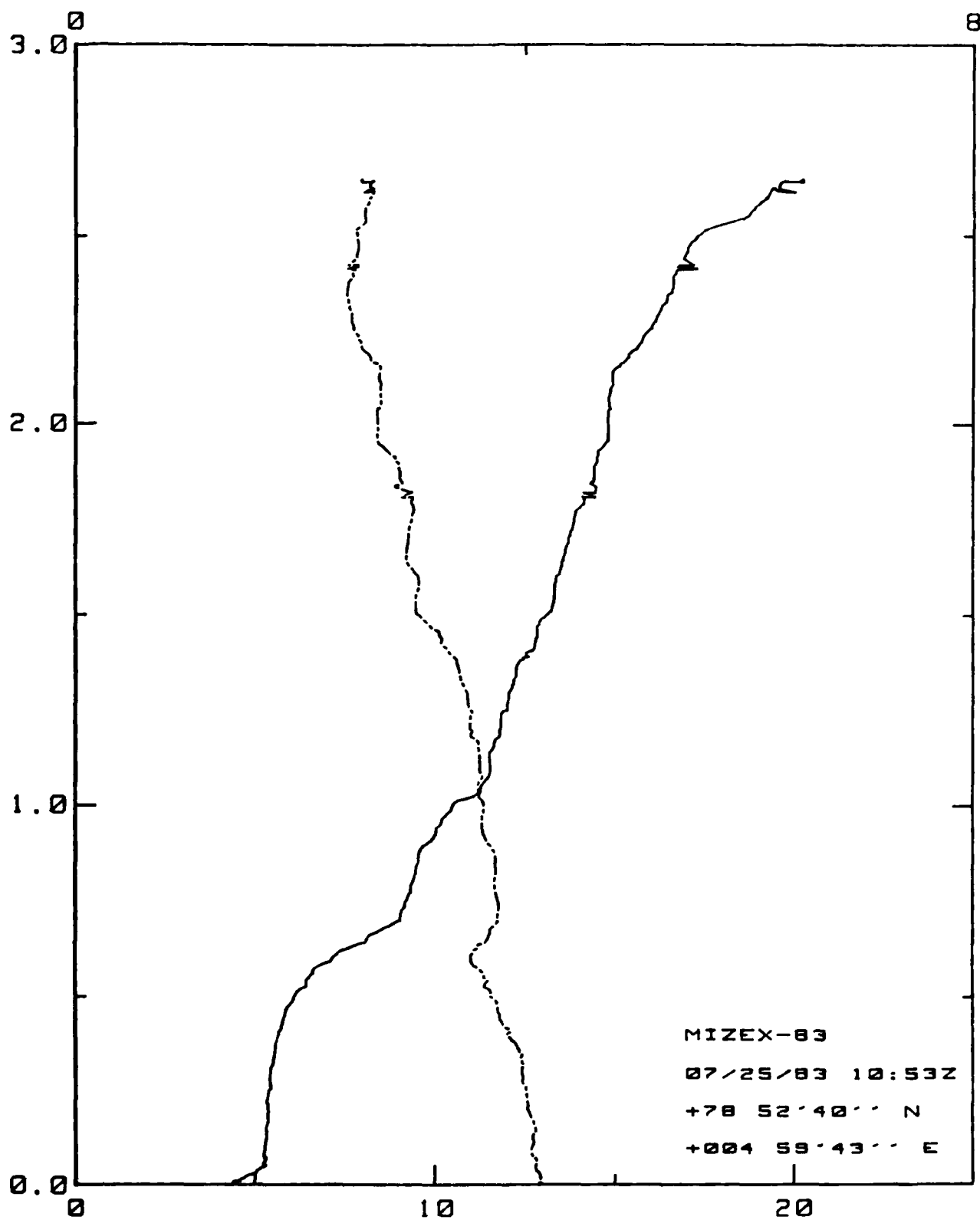
07/16/83 16:04Z

+78 29'25'' N

+011 32'48'' E

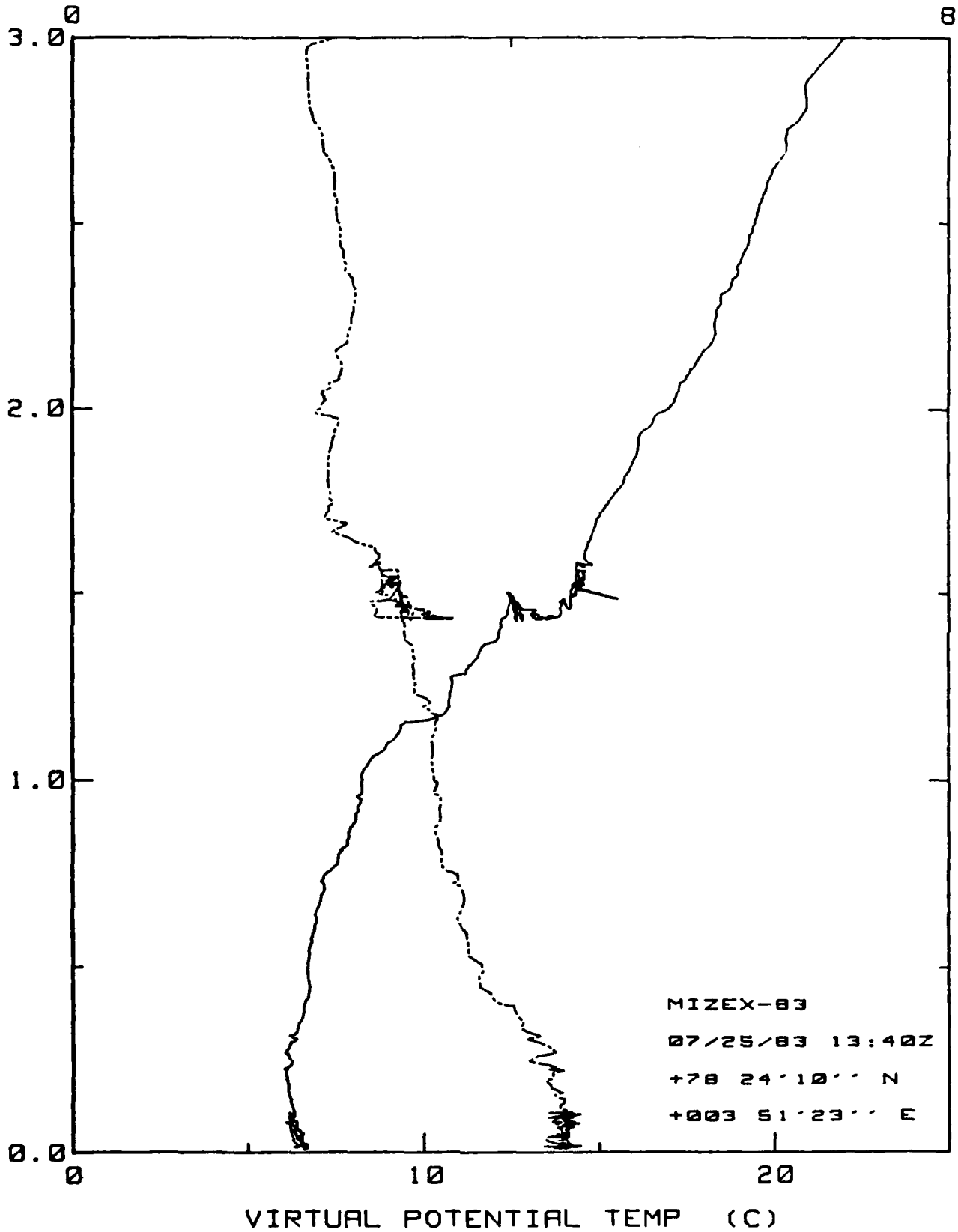
VIRTUAL POTENTIAL TEMP (C)

Q SPECIFIC HUMIDITY (g/Kg)

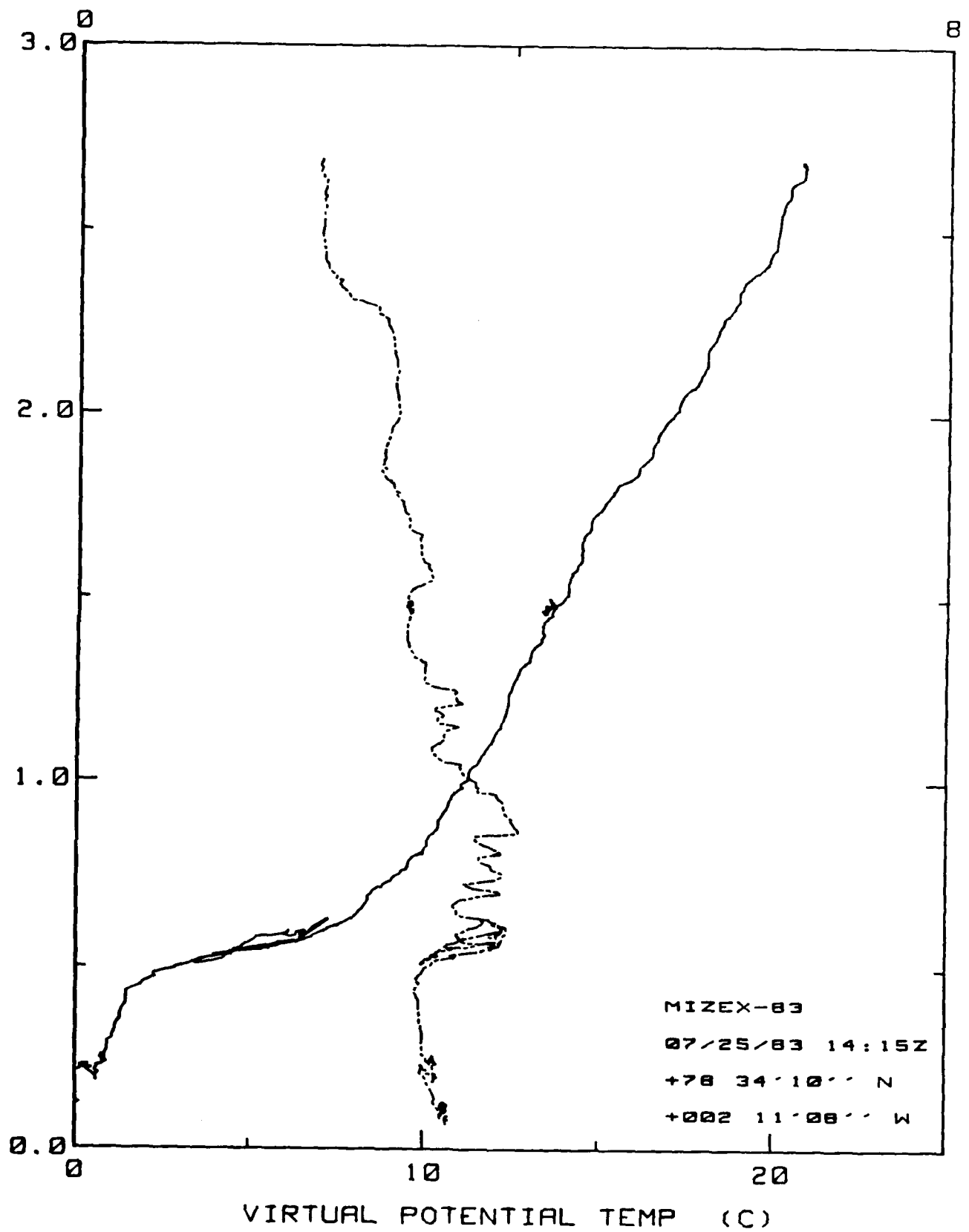


VIRTUAL POTENTIAL TEMP (C)

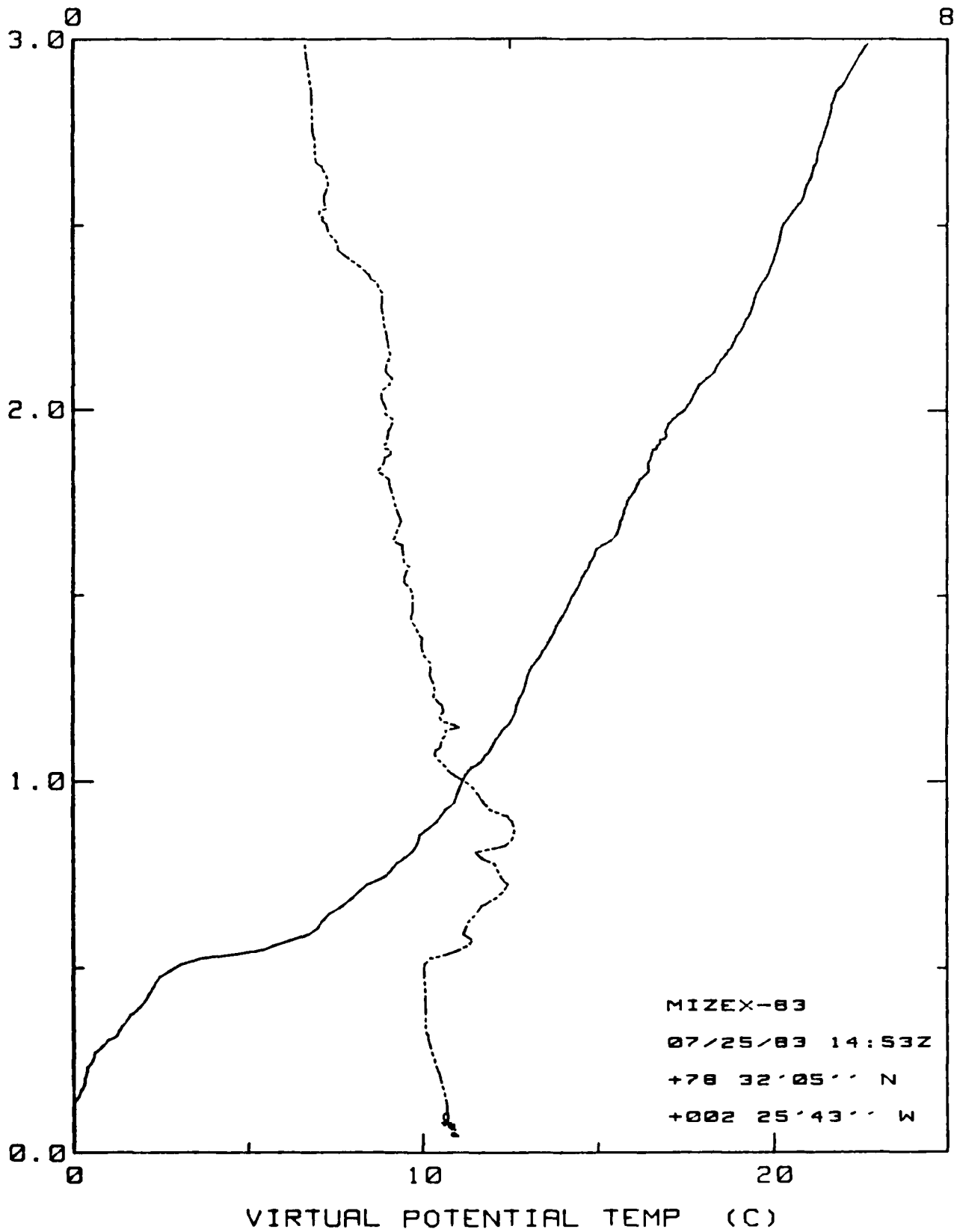
Q SPECIFIC HUMIDITY (g/Kg)



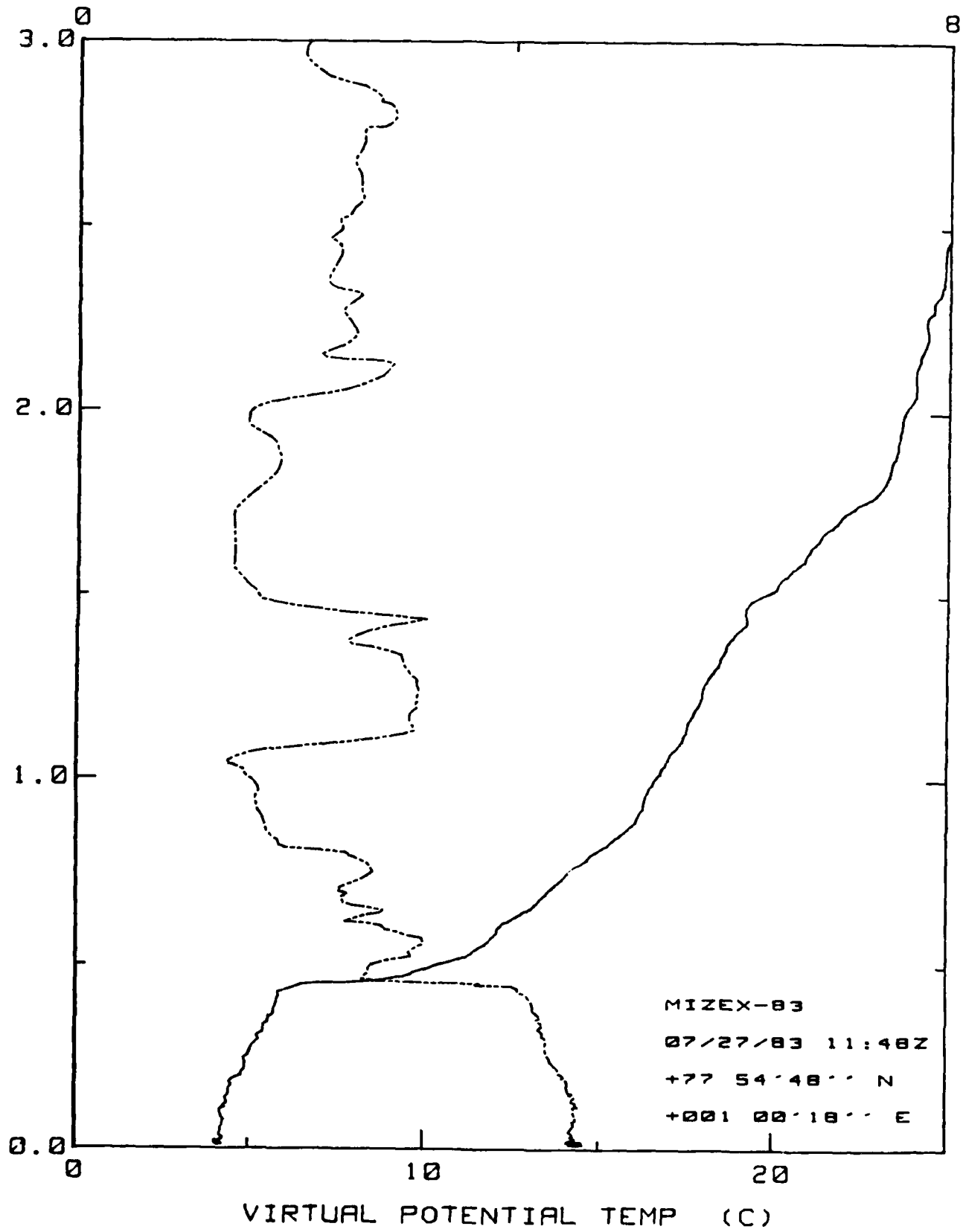
Q SPECIFIC HUMIDITY (g/Kg)



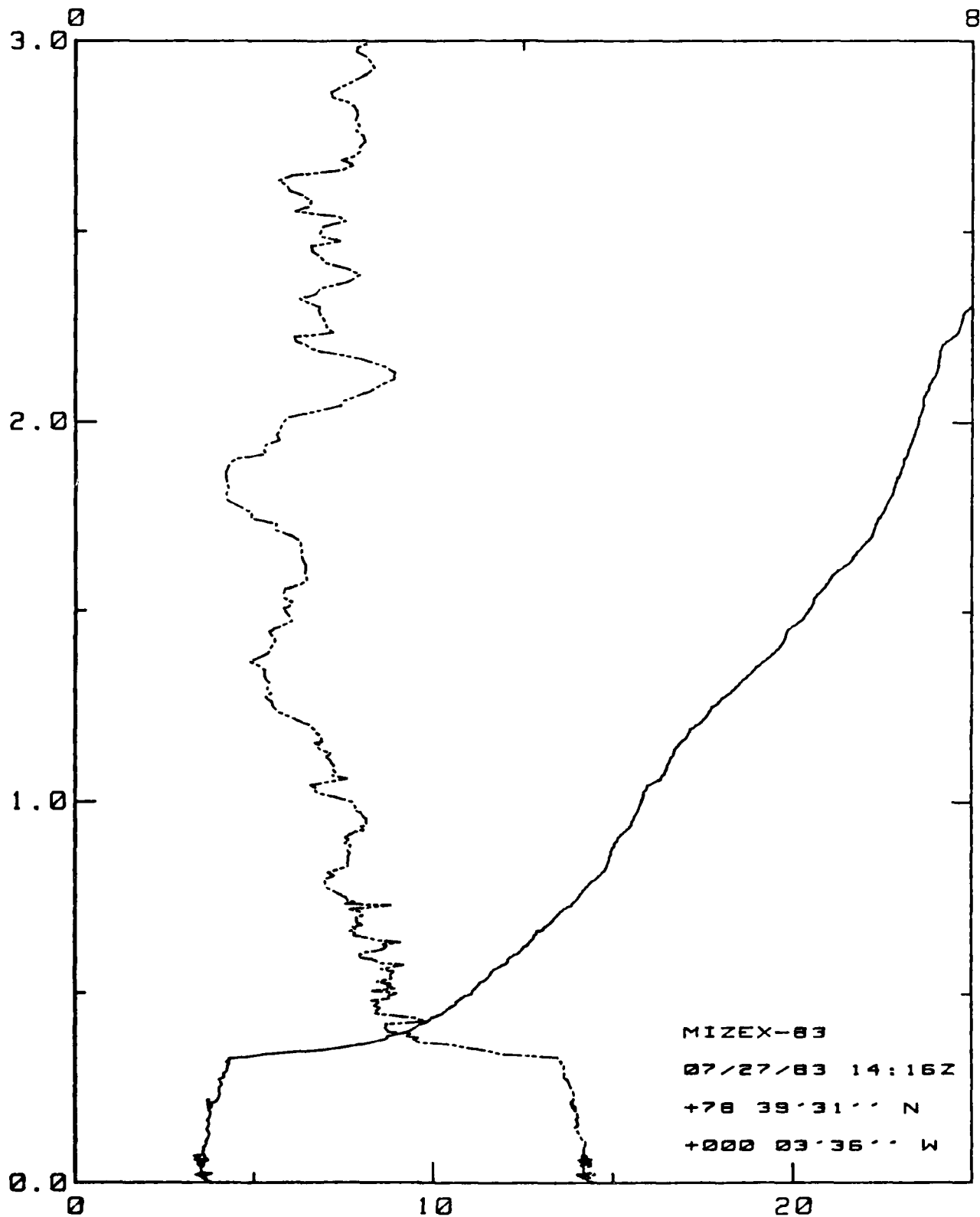
Q SPECIFIC HUMIDITY (g/Kg)



Q SPECIFIC HUMIDITY (g/Kg)

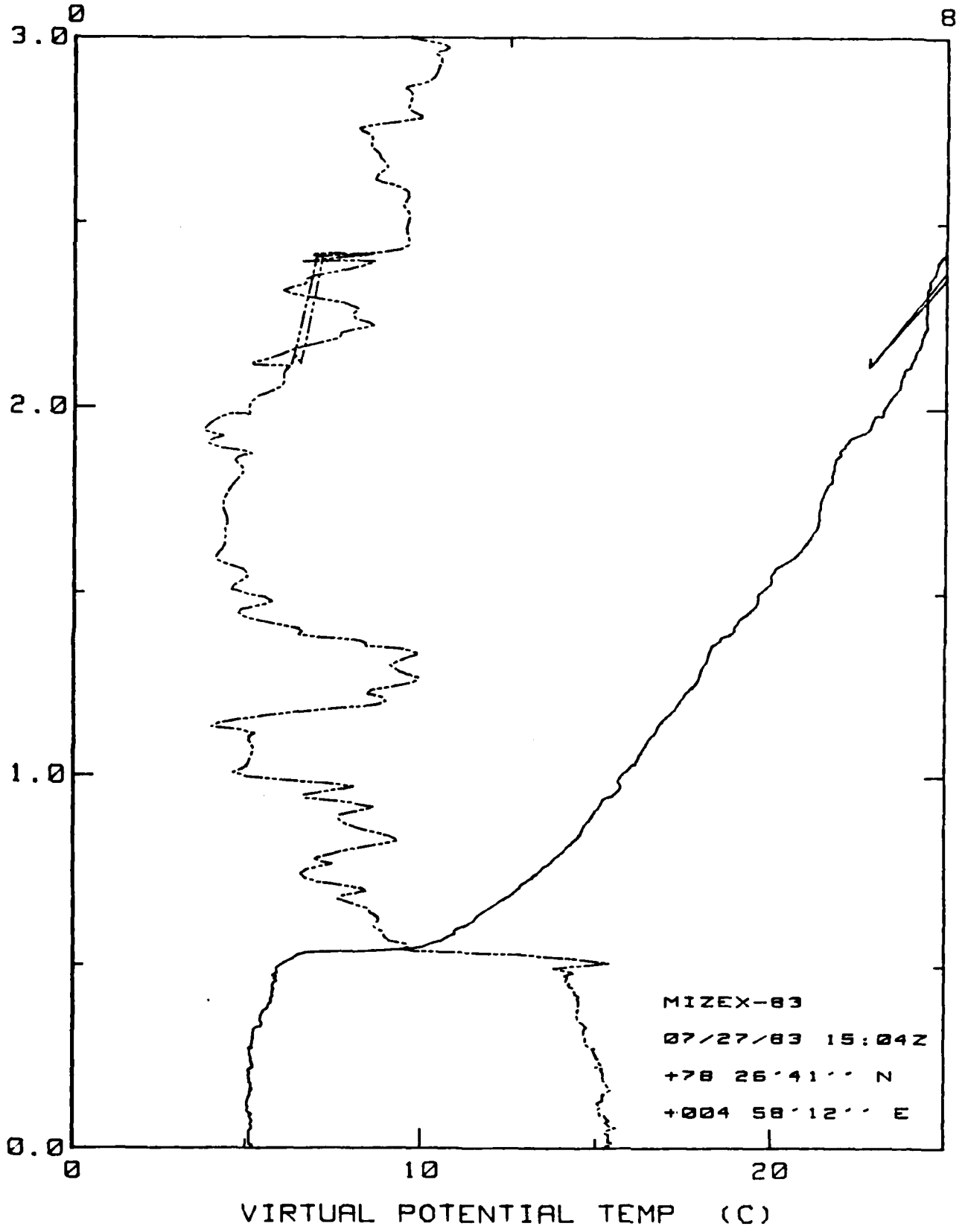


Q SPECIFIC HUMIDITY (g/Kg)

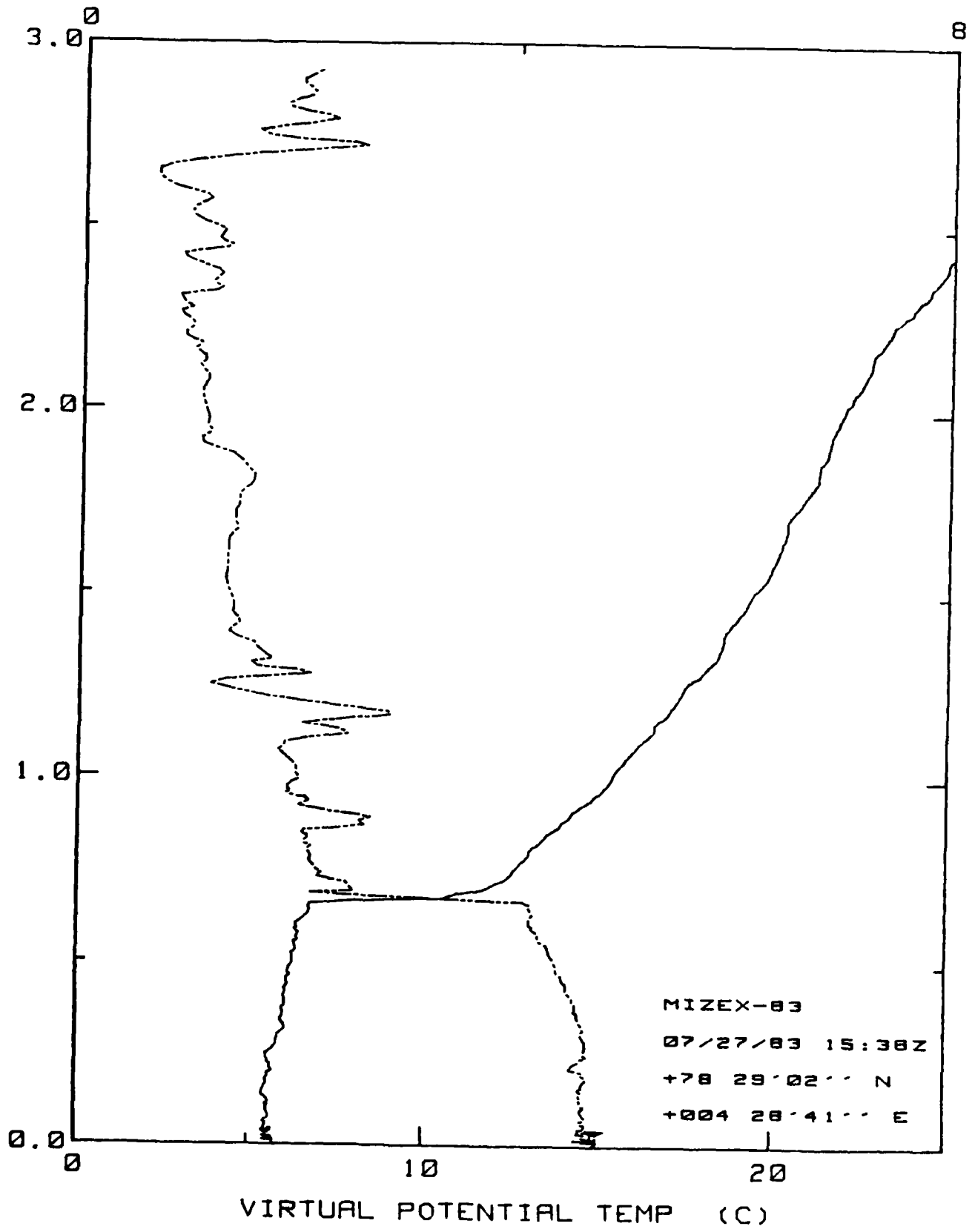


VIRTUAL POTENTIAL TEMP (C)

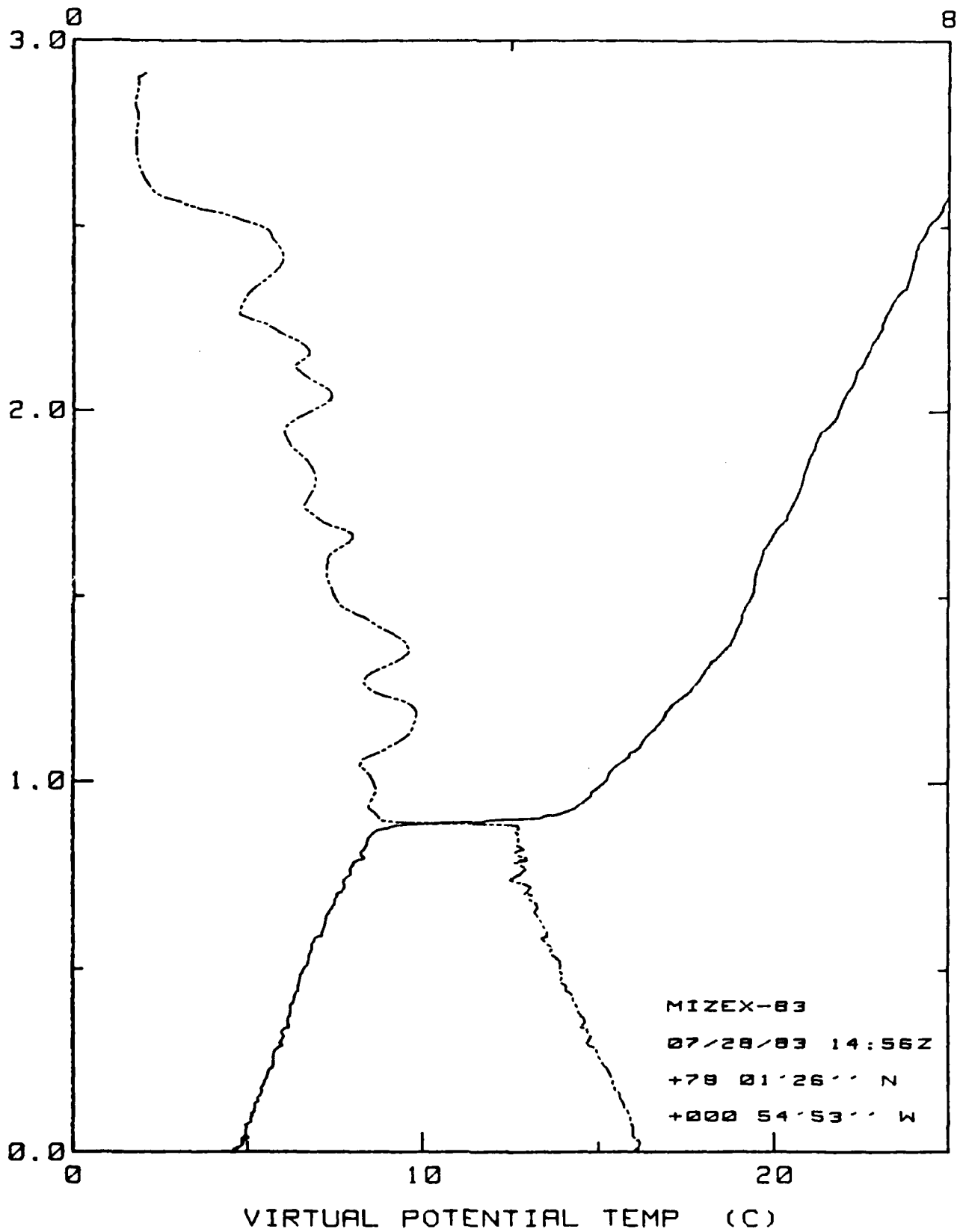
Q SPECIFIC HUMIDITY (g/Kg)



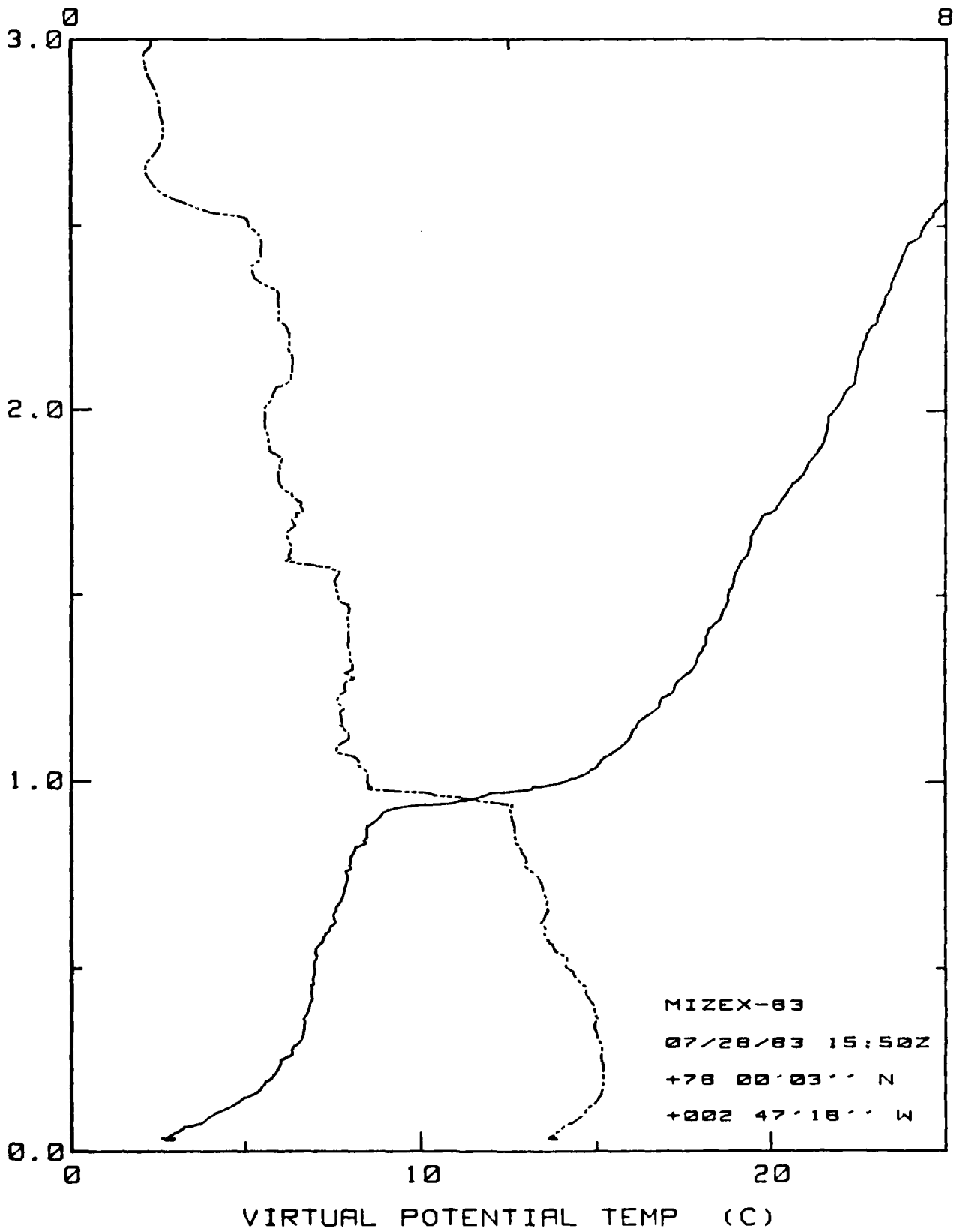
Q SPECIFIC HUMIDITY (g/Kg)



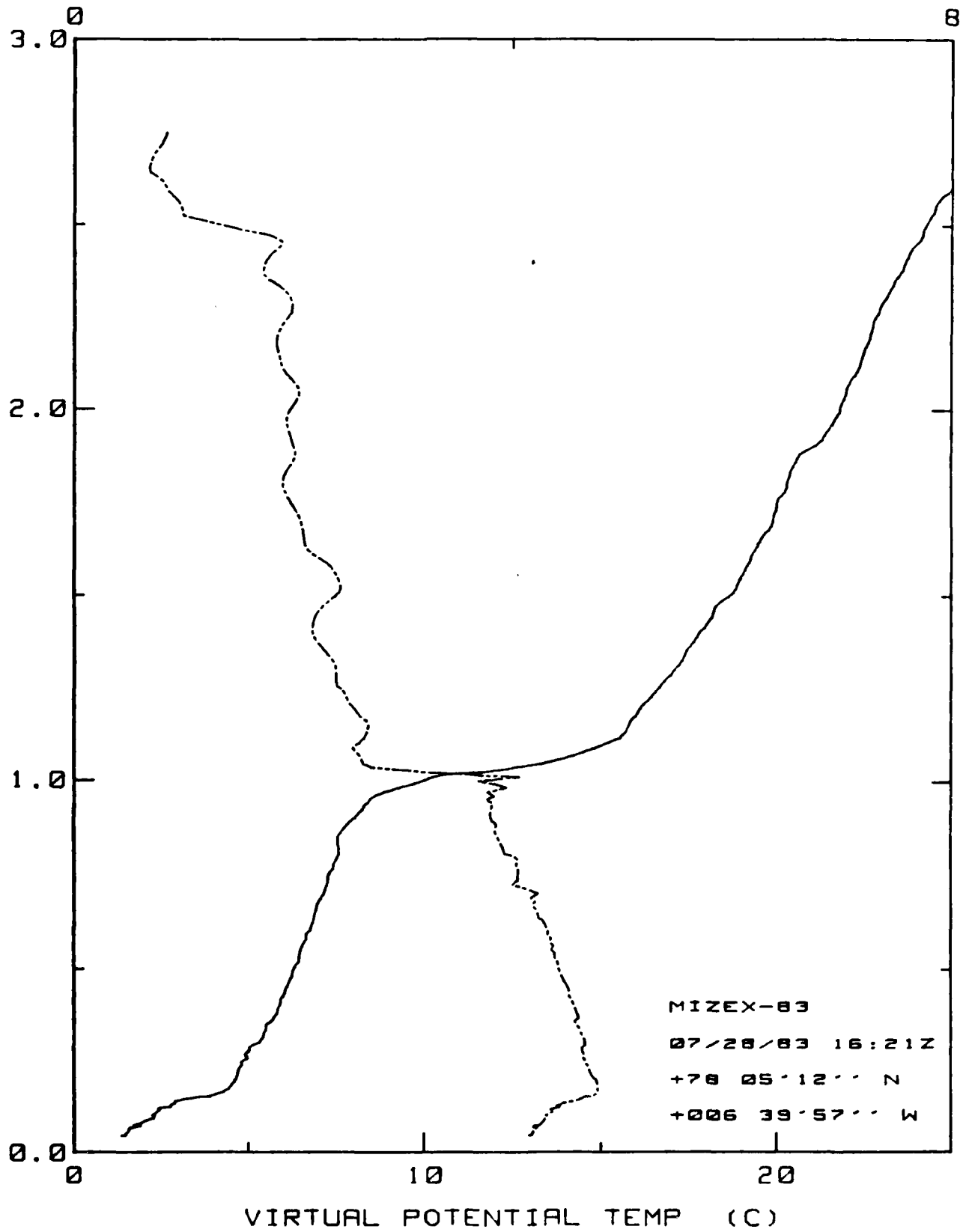
Q SPECIFIC HUMIDITY (g/Kg)



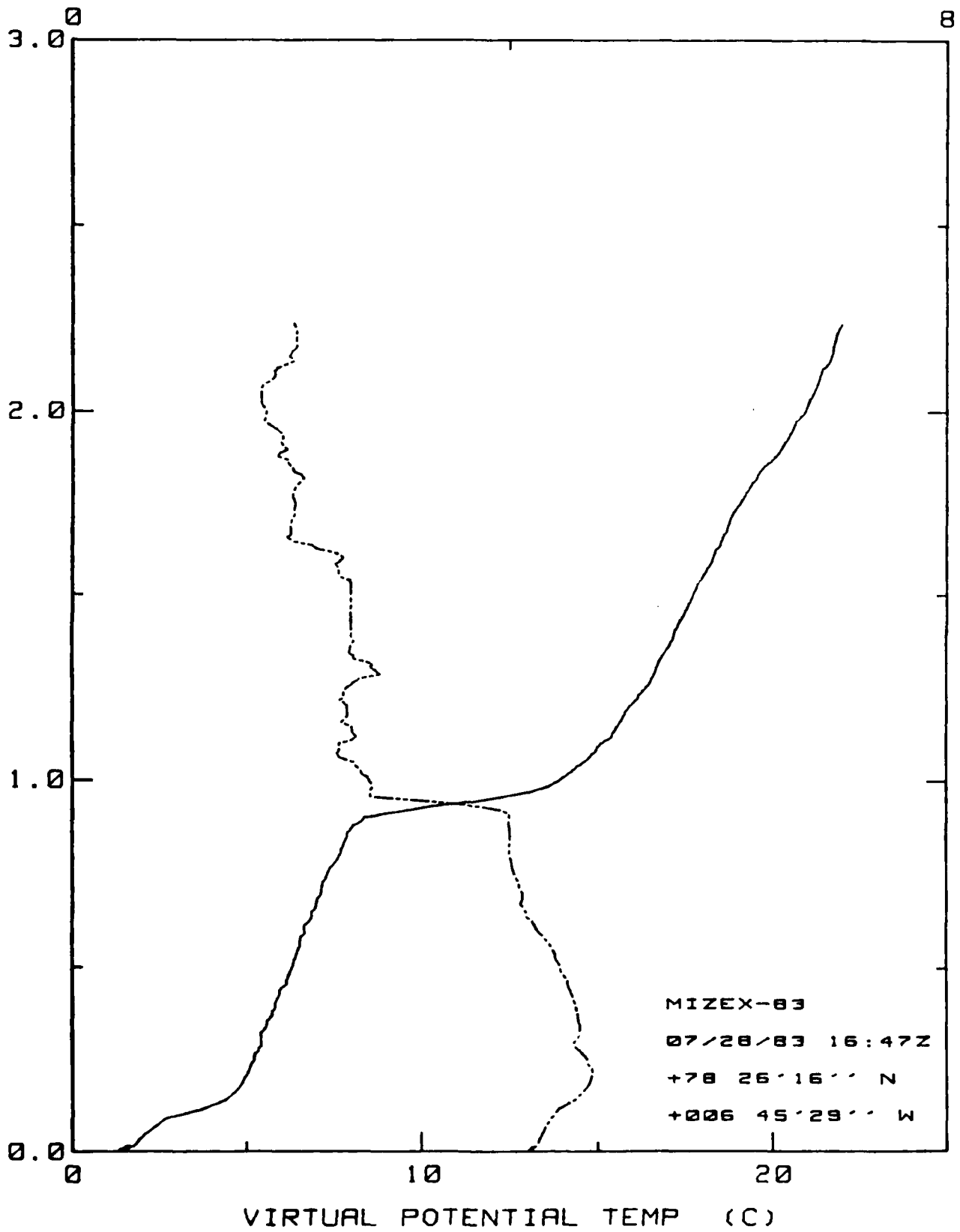
Q SPECIFIC HUMIDITY (g/Kg)



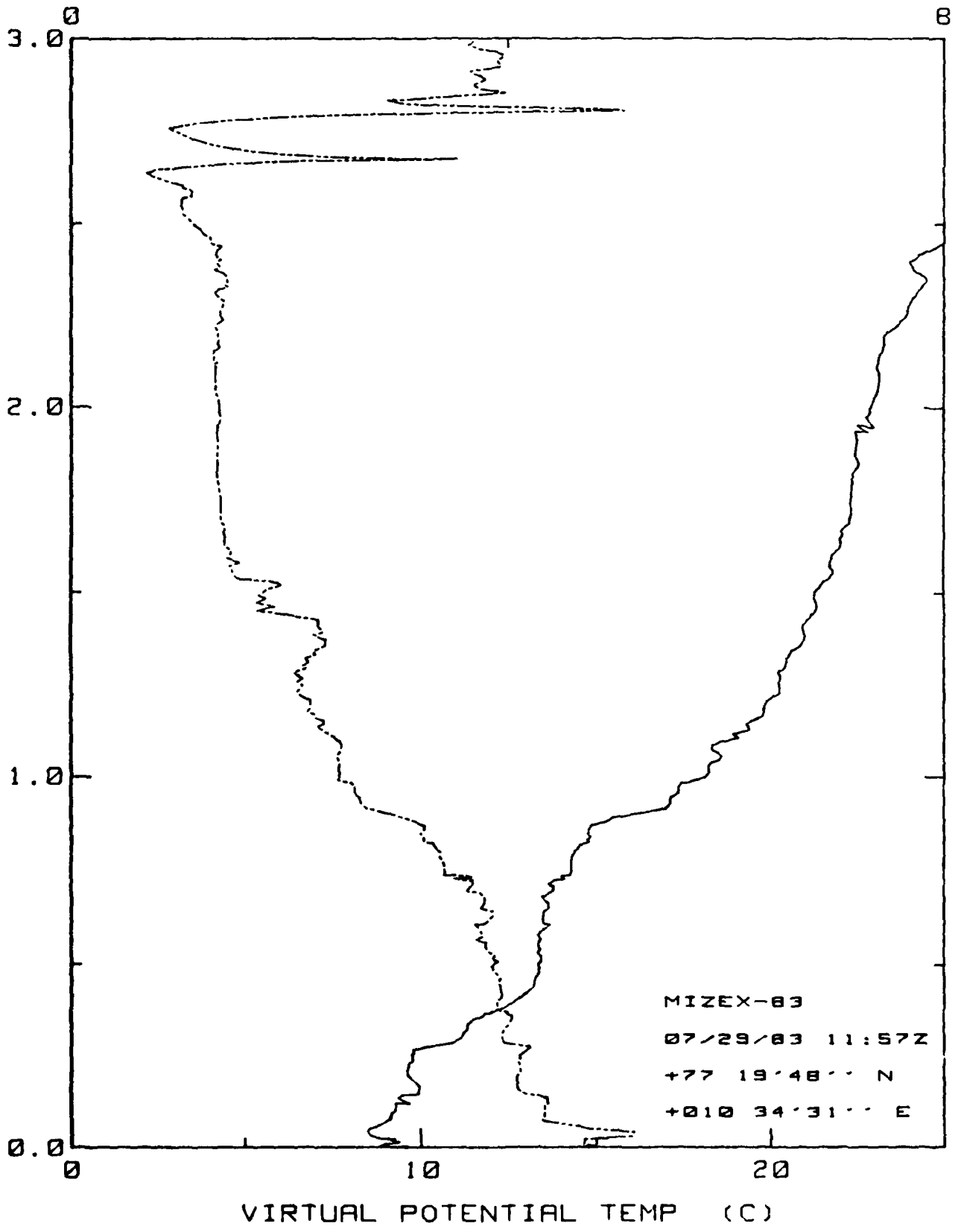
Q SPECIFIC HUMIDITY (g/Kg)



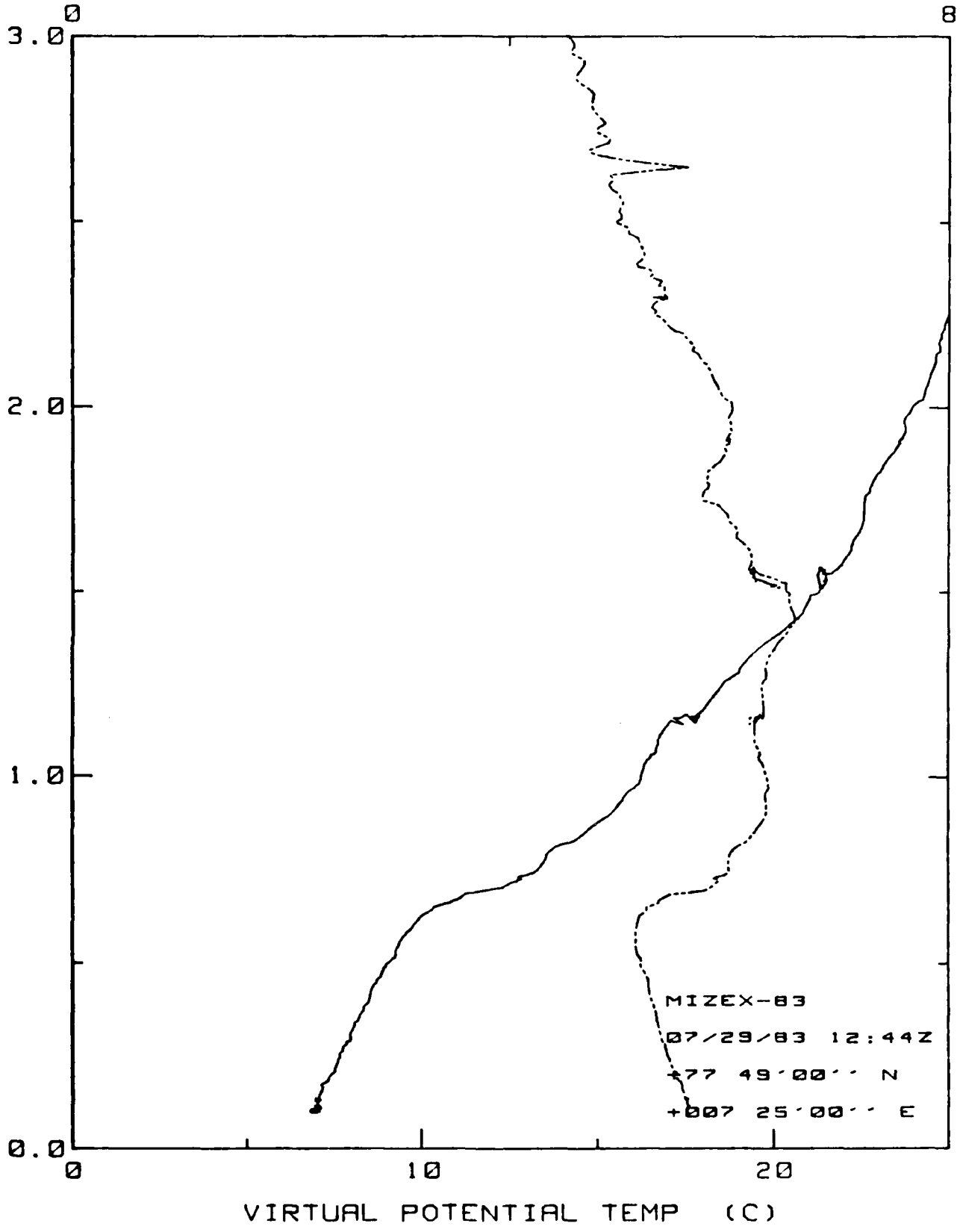
Q SPECIFIC HUMIDITY (g/Kg)



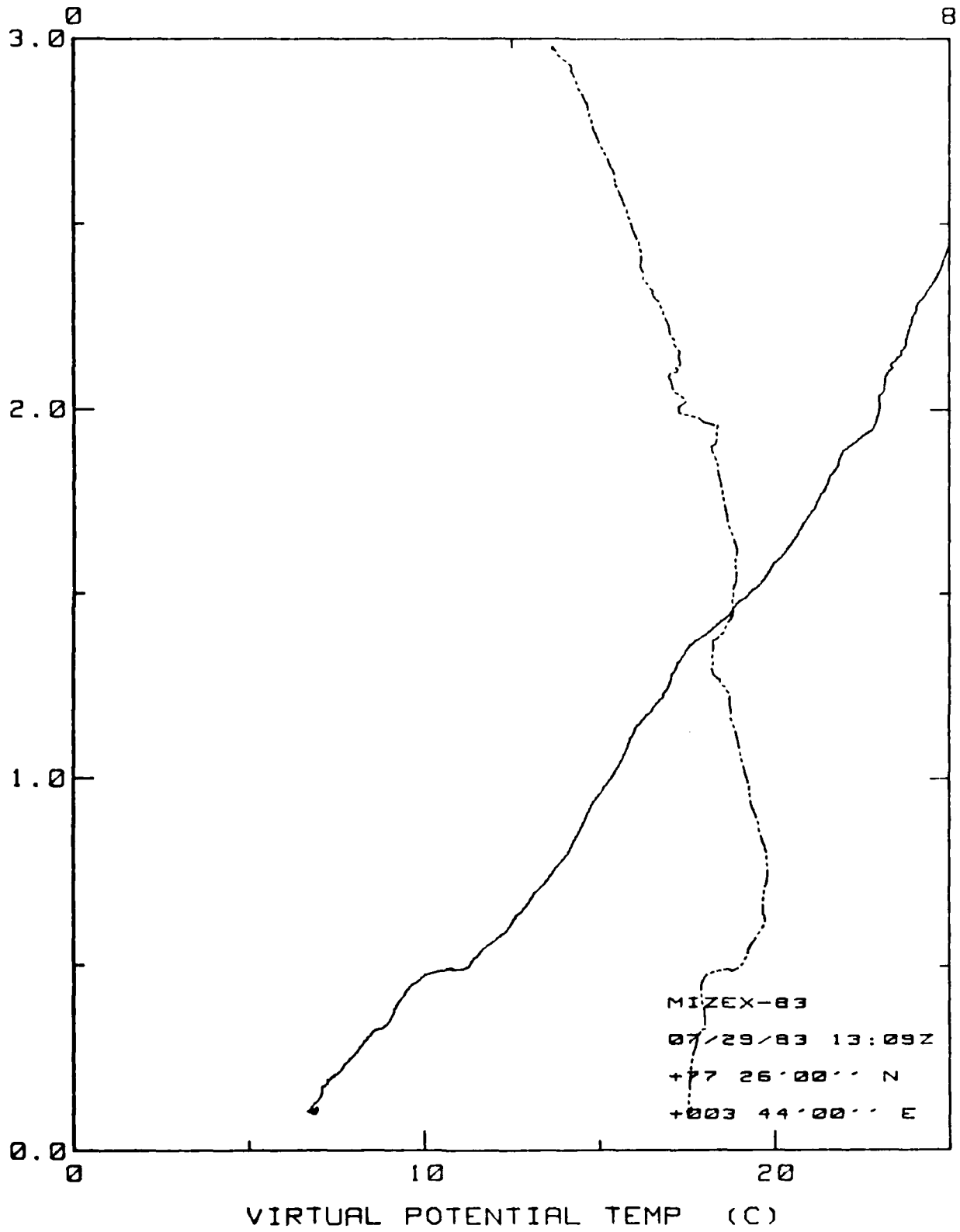
Q SPECIFIC HUMIDITY (g/Kg)



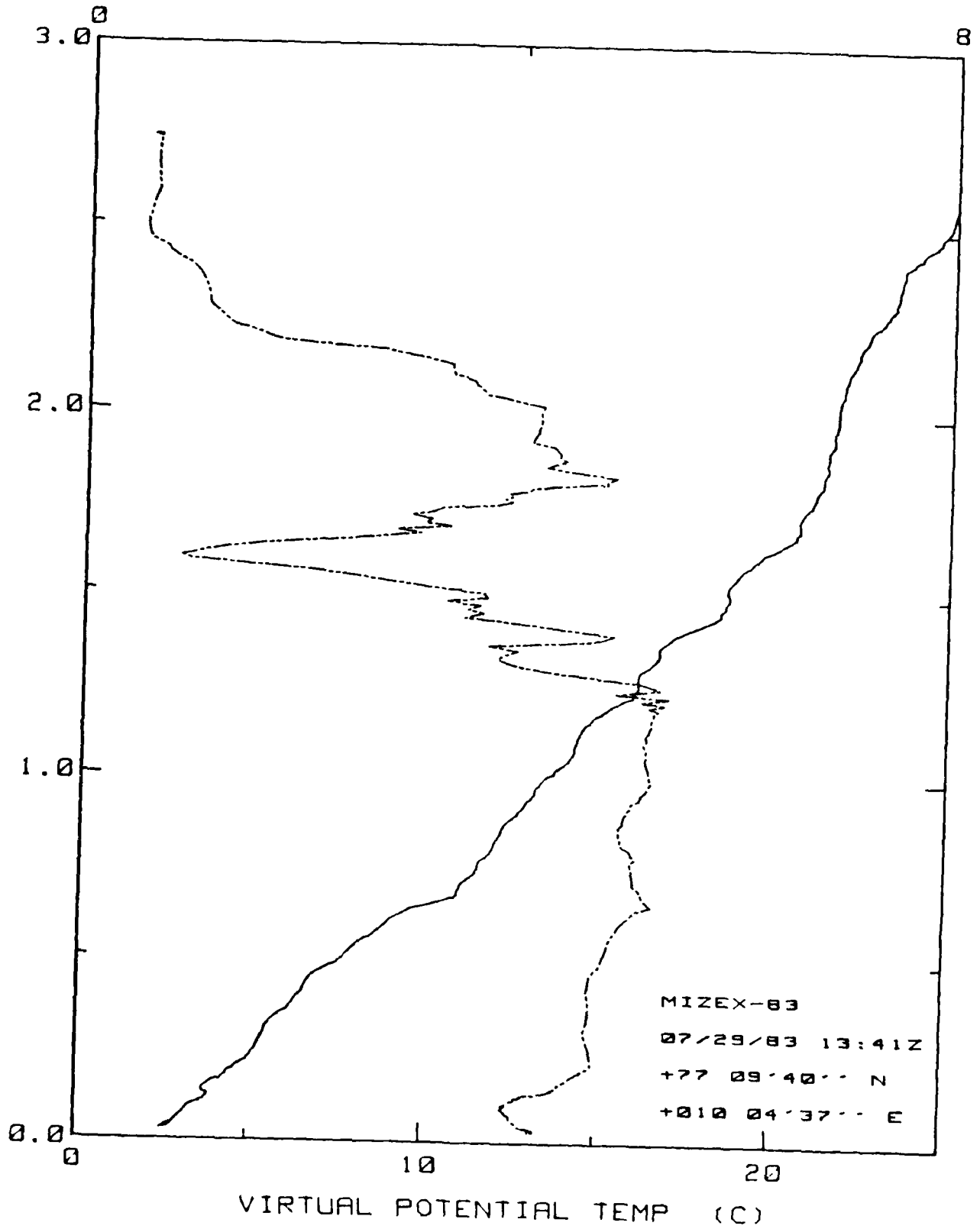
Q SPECIFIC HUMIDITY (g/Kg)



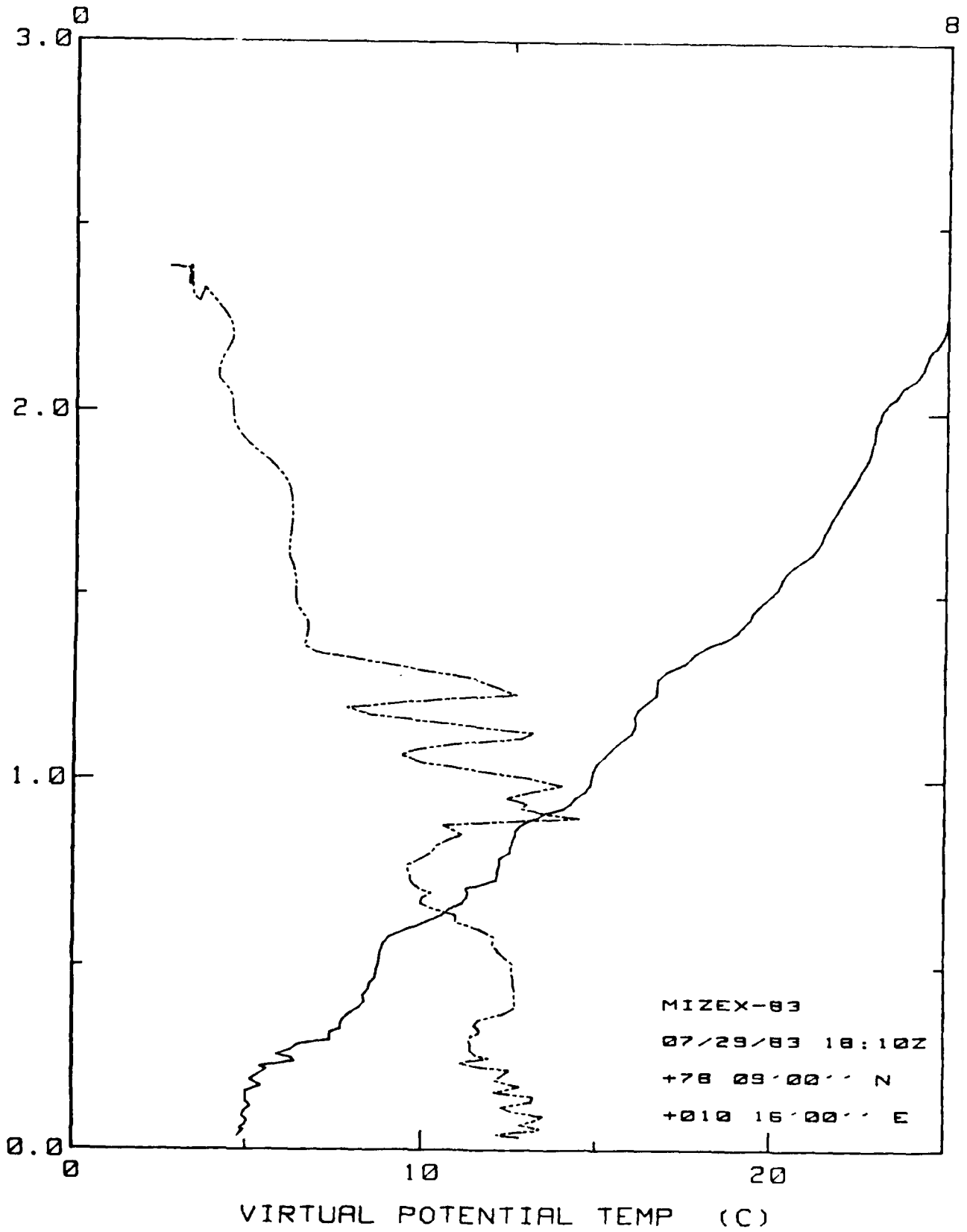
Q SPECIFIC HUMIDITY (g/Kg)



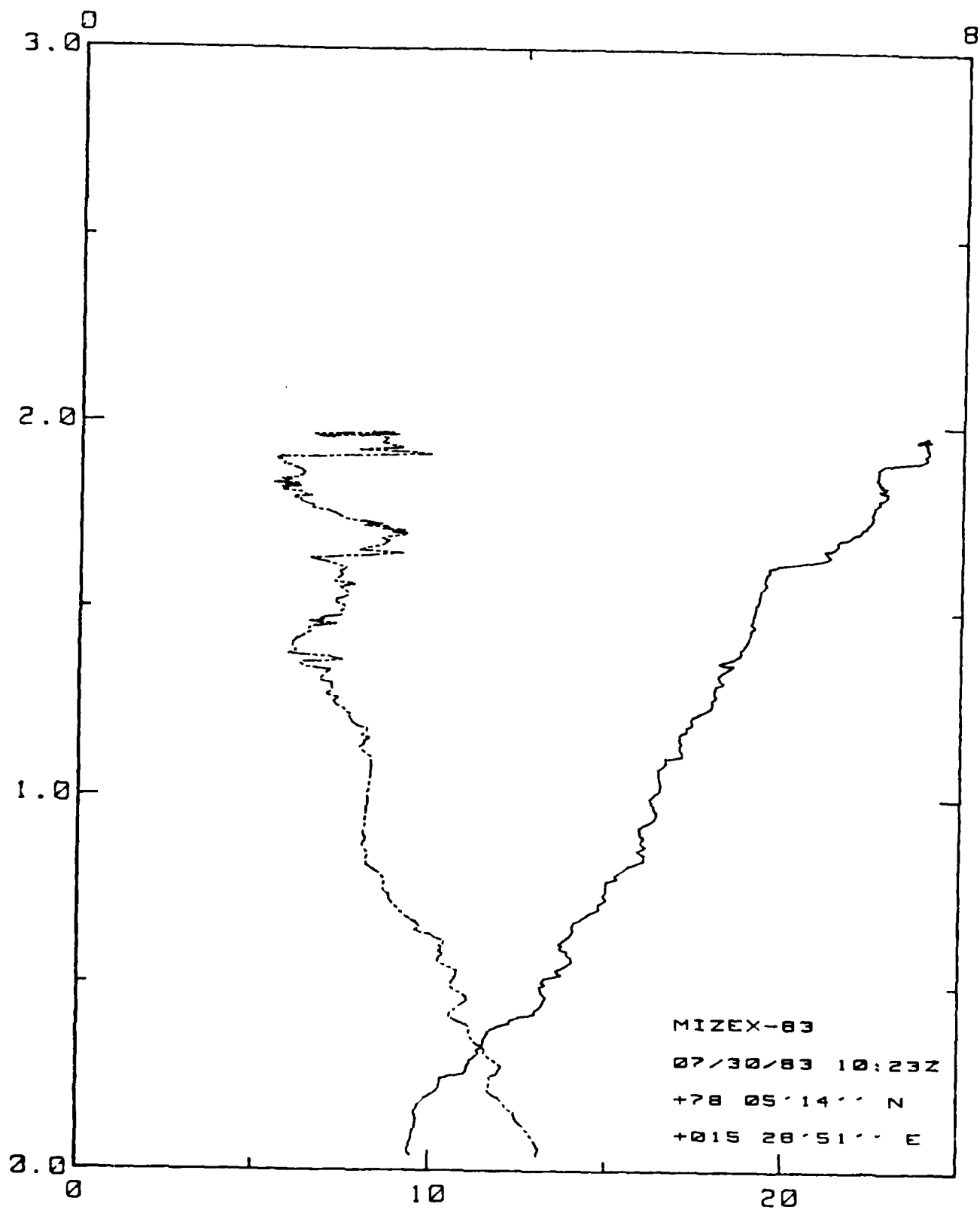
Q SPECIFIC HUMIDITY (g/Kg)



Q SPECIFIC HUMIDITY (g/Kg)

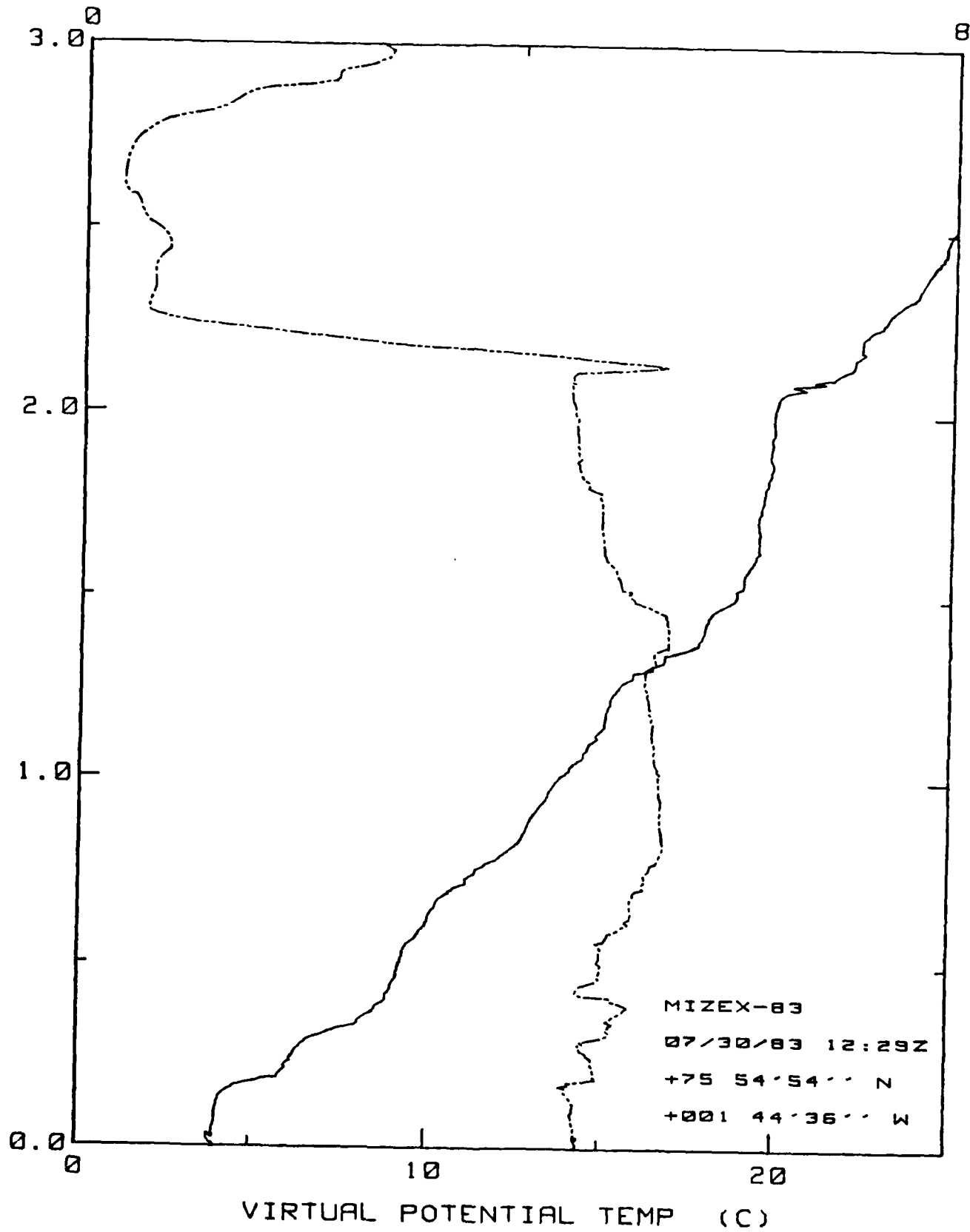


Q SPECIFIC HUMIDITY (g/Kg)

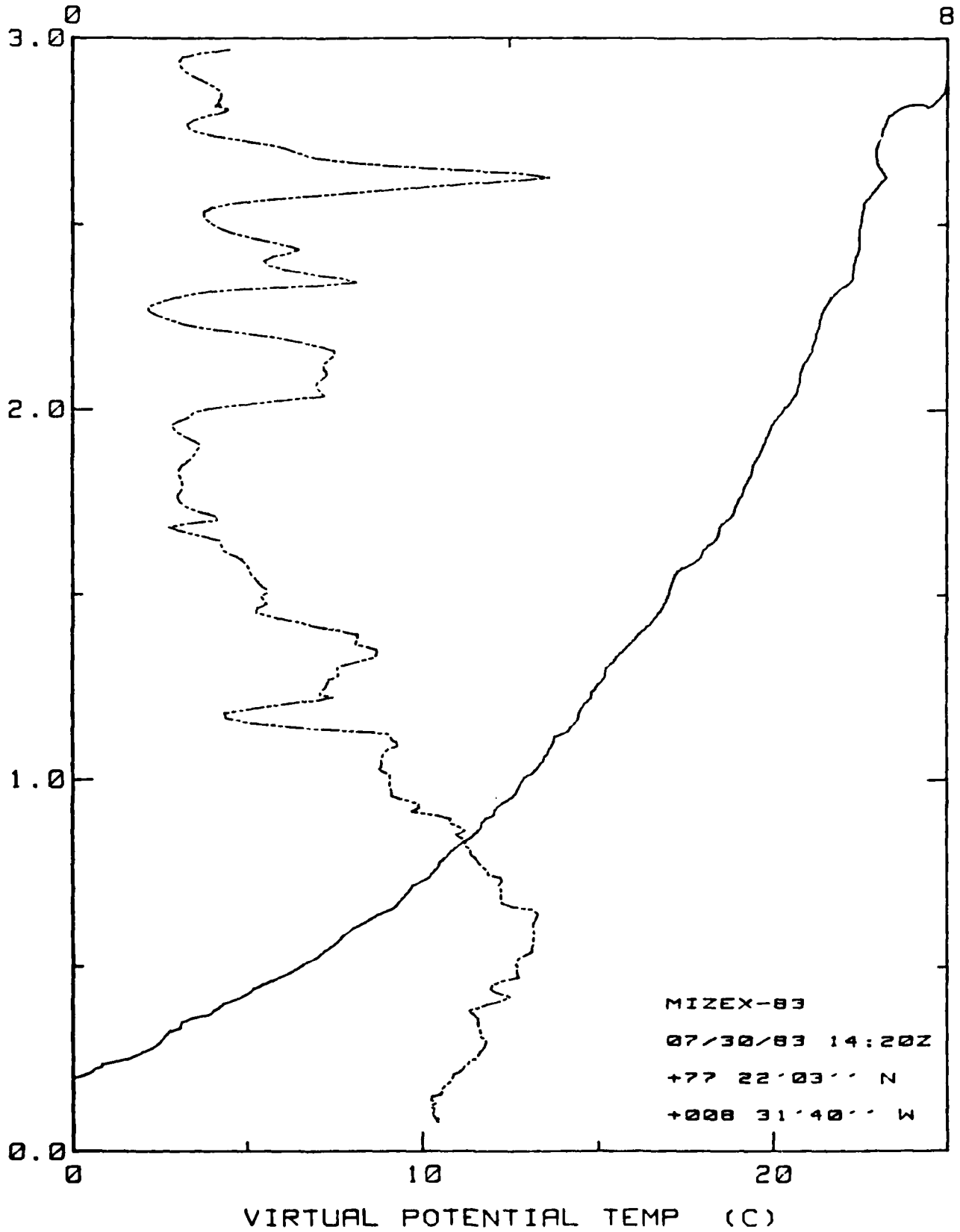


VIRTUAL POTENTIAL TEMP (C)

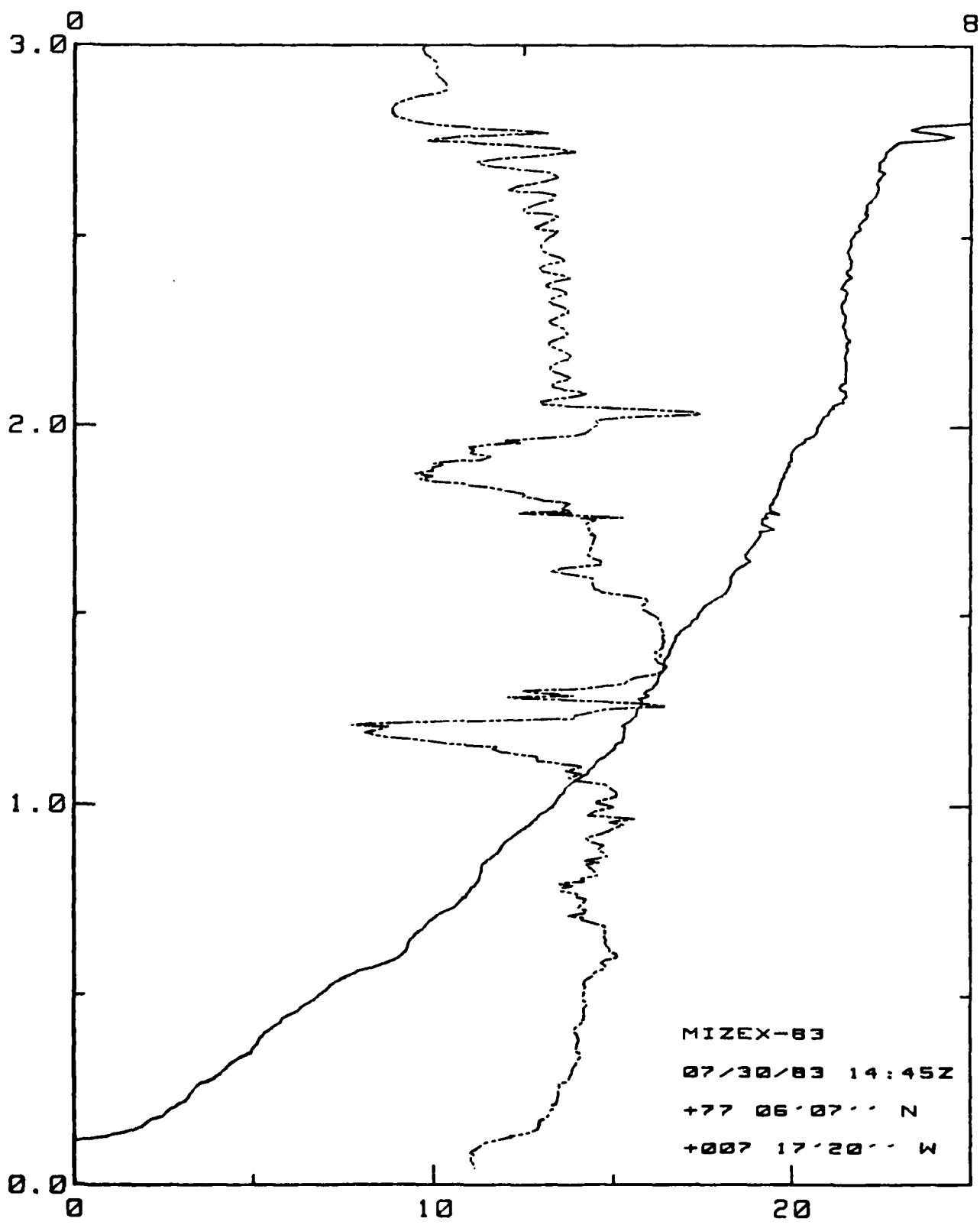
Q SPECIFIC HUMIDITY (g/Kg)



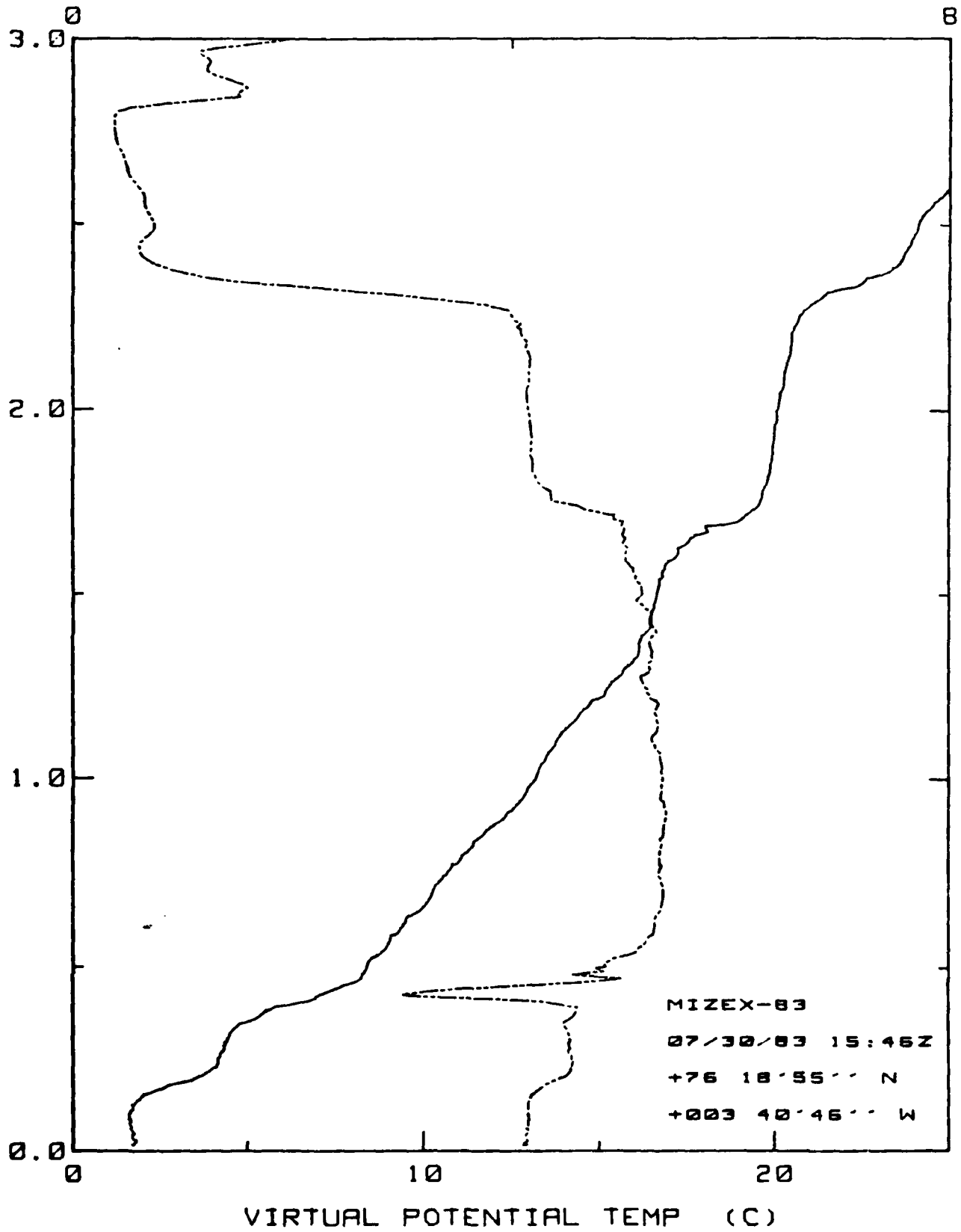
Q SPECIFIC HUMIDITY (g/Kg)



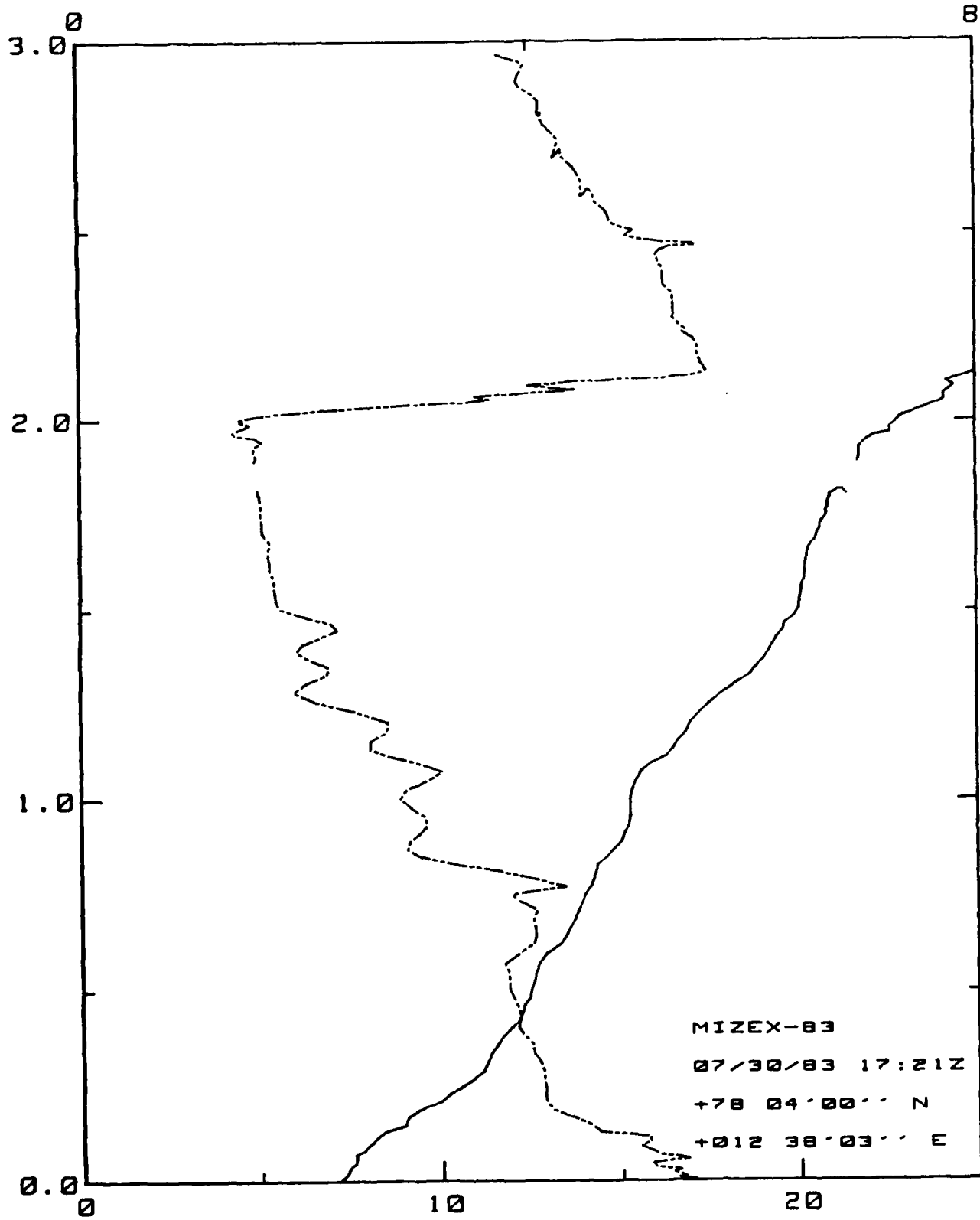
Q SPECIFIC HUMIDITY (g/Kg)



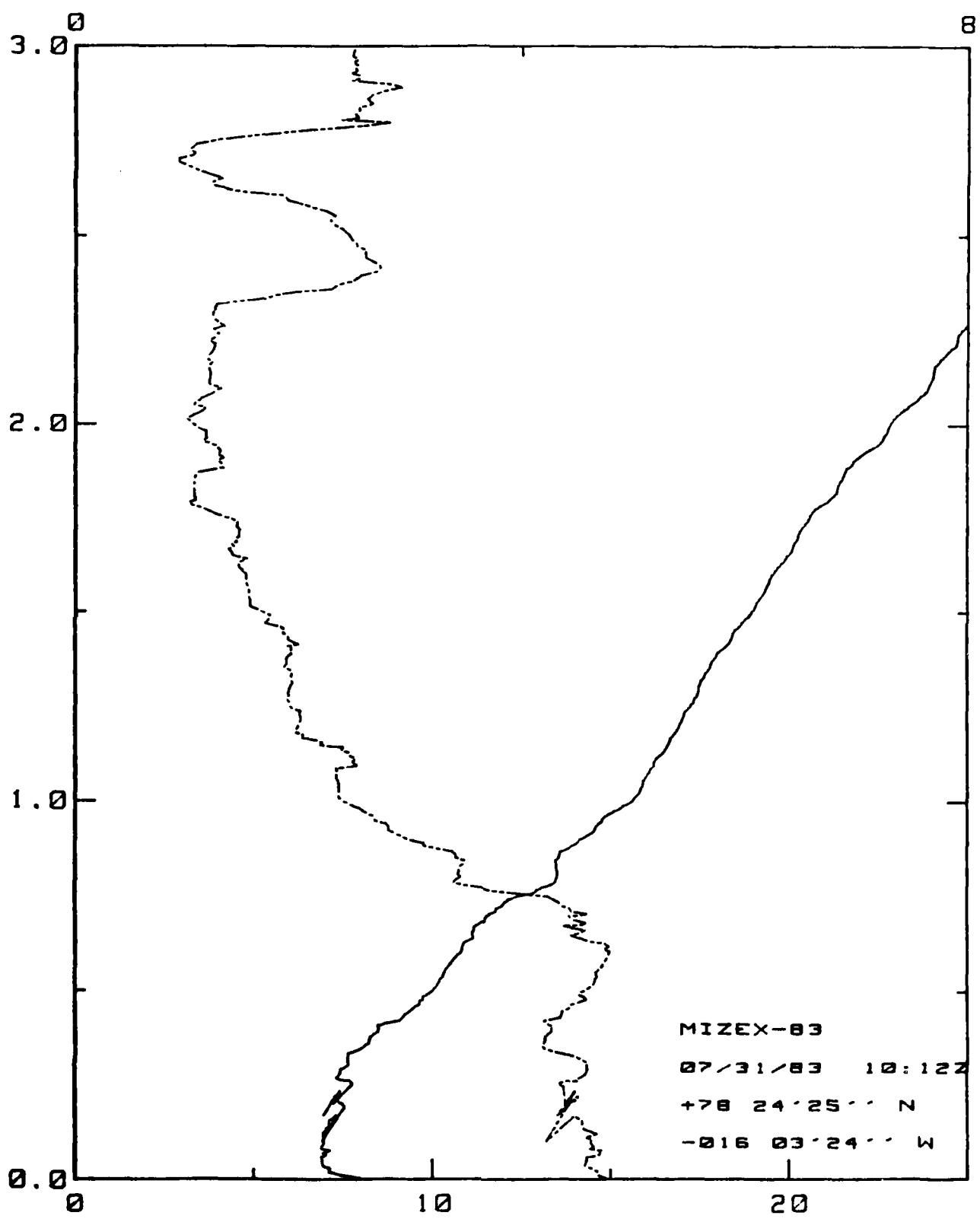
Q SPECIFIC HUMIDITY (g/Kg)



Q SPECIFIC HUMIDITY (g/Kg)



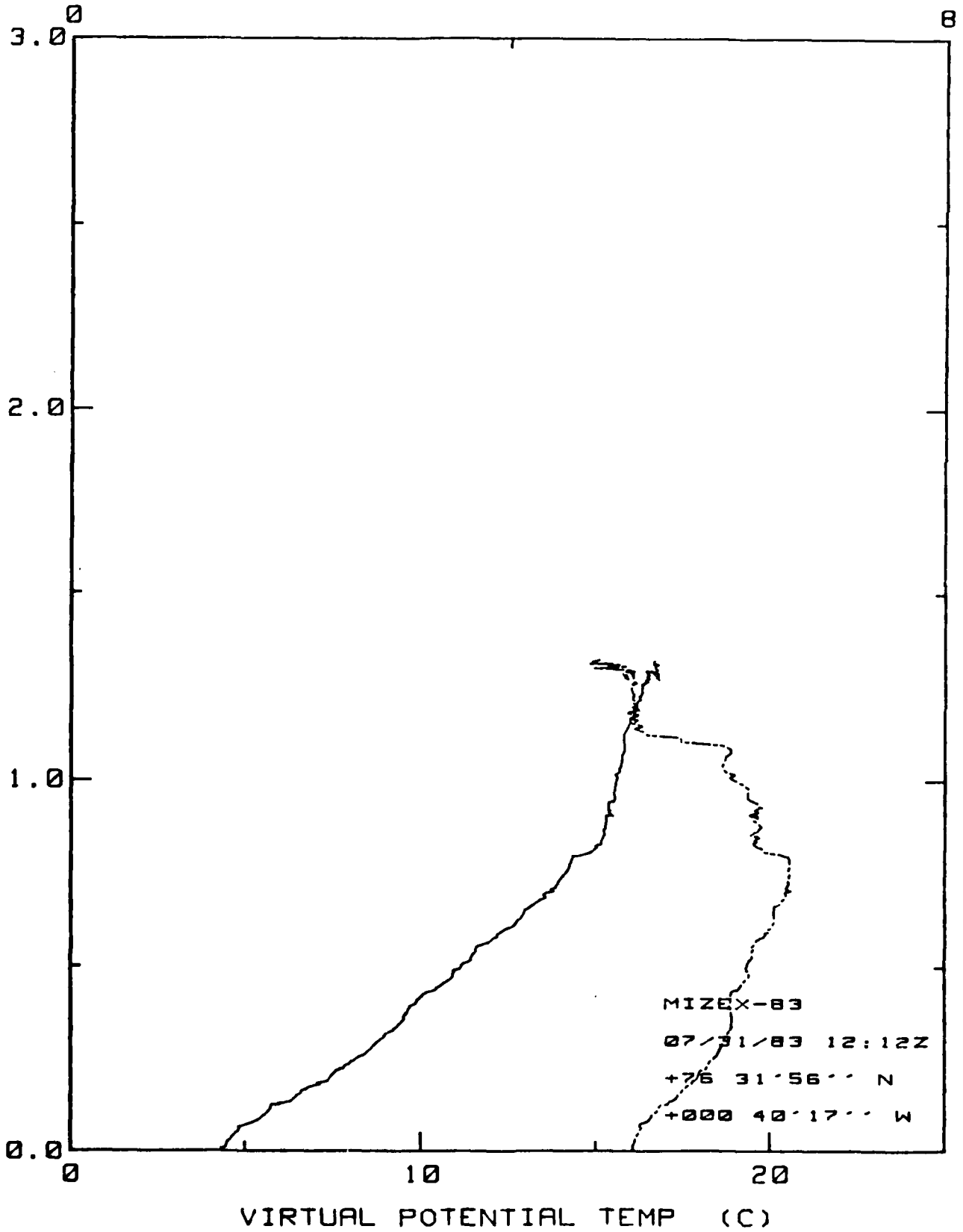
Q SPECIFIC HUMIDITY (g/Kg)



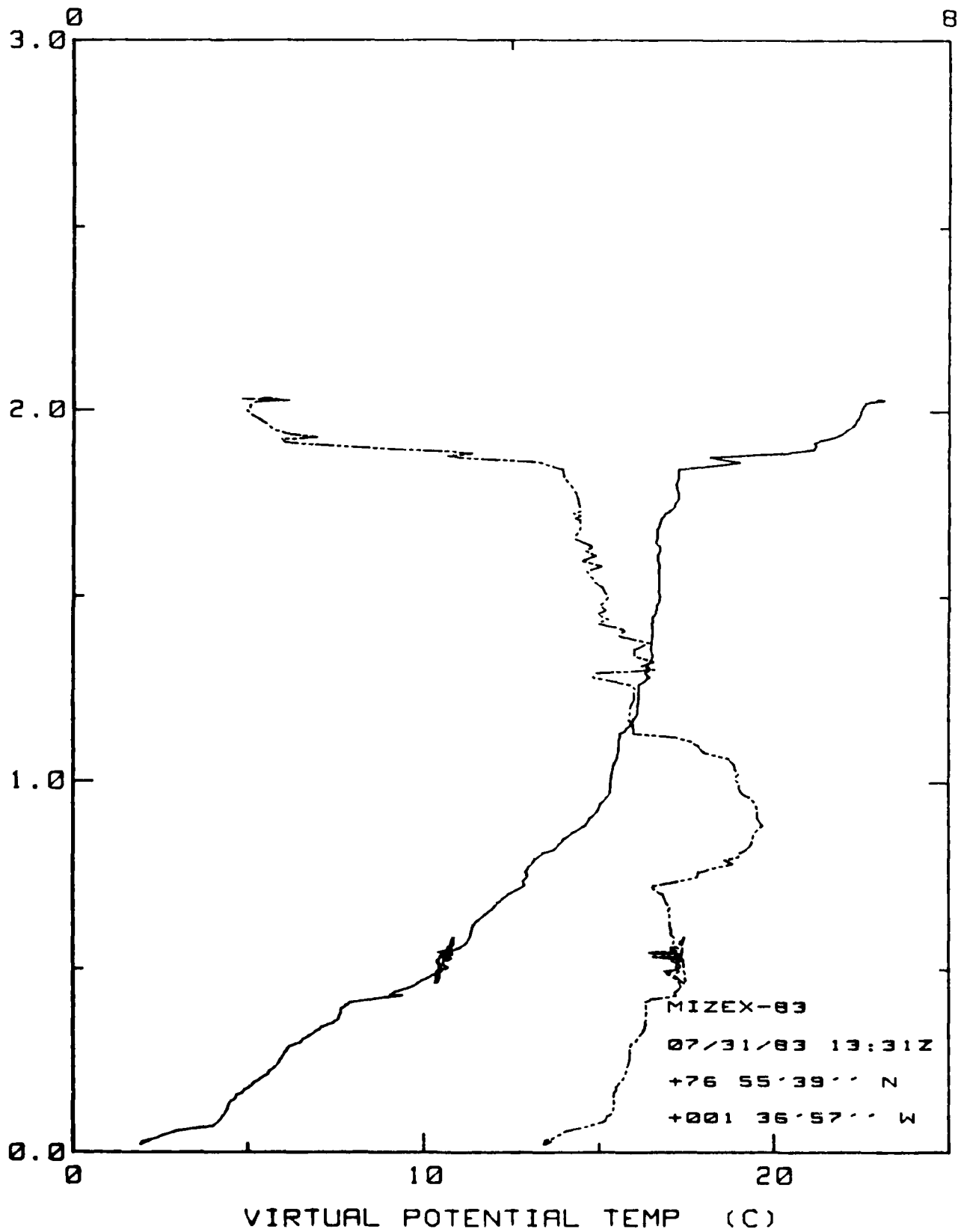
MIZEX-03
07/31/83 10:12Z
+78 24'25" N
-016 03'24" W

VIRTUAL POTENTIAL TEMP (C)

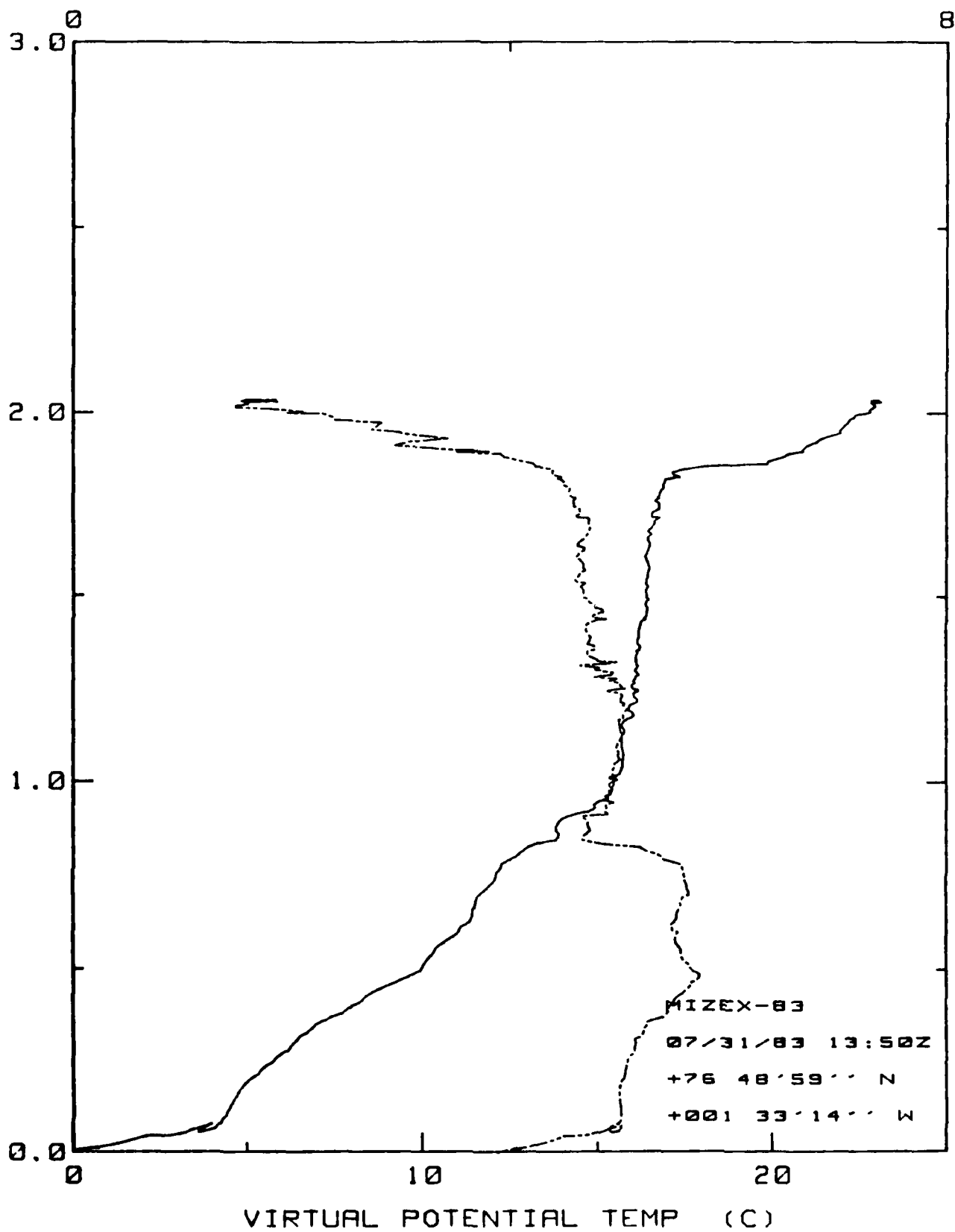
Q SPECIFIC HUMIDITY (g/Kg)



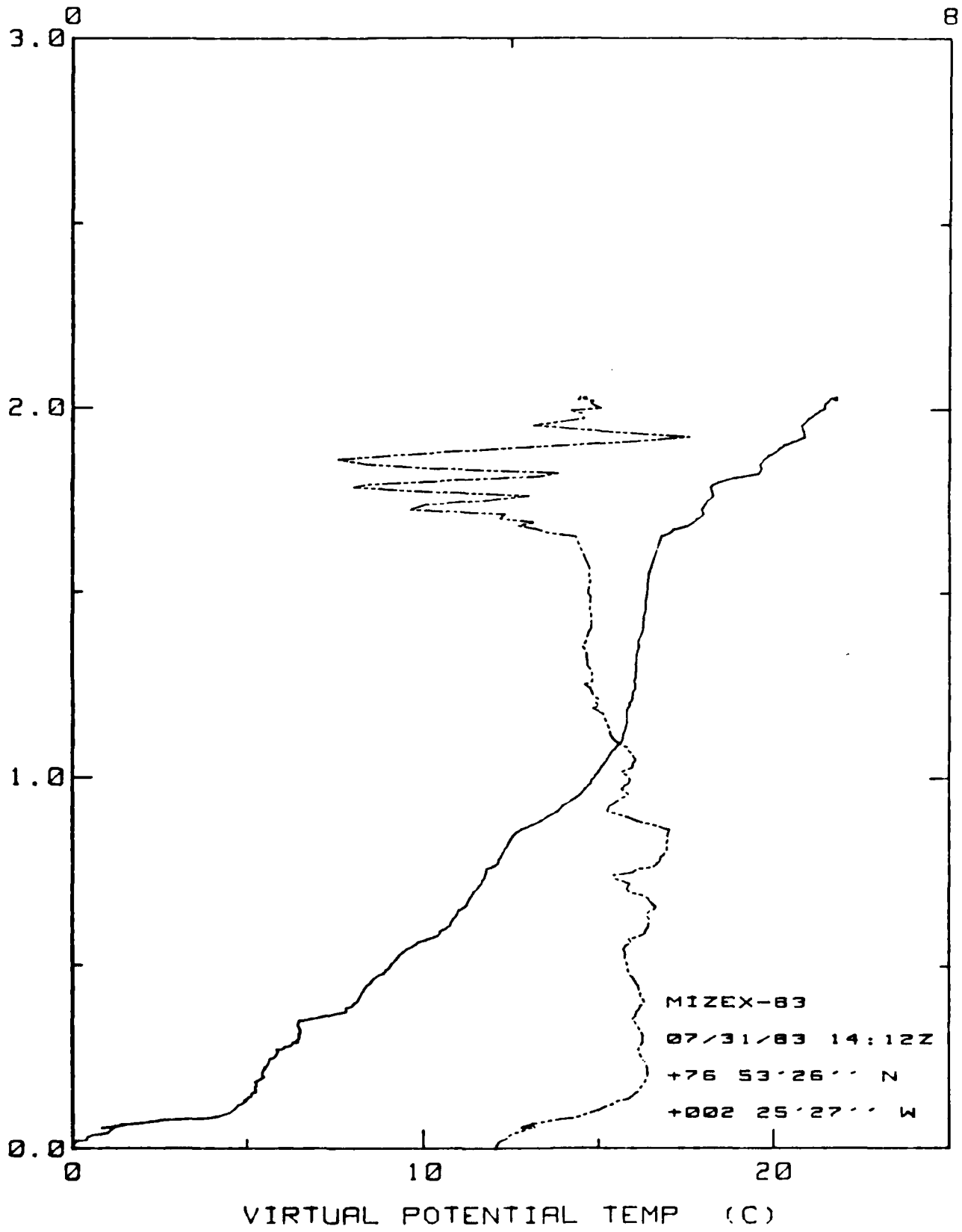
Q SPECIFIC HUMIDITY (g/Kg)



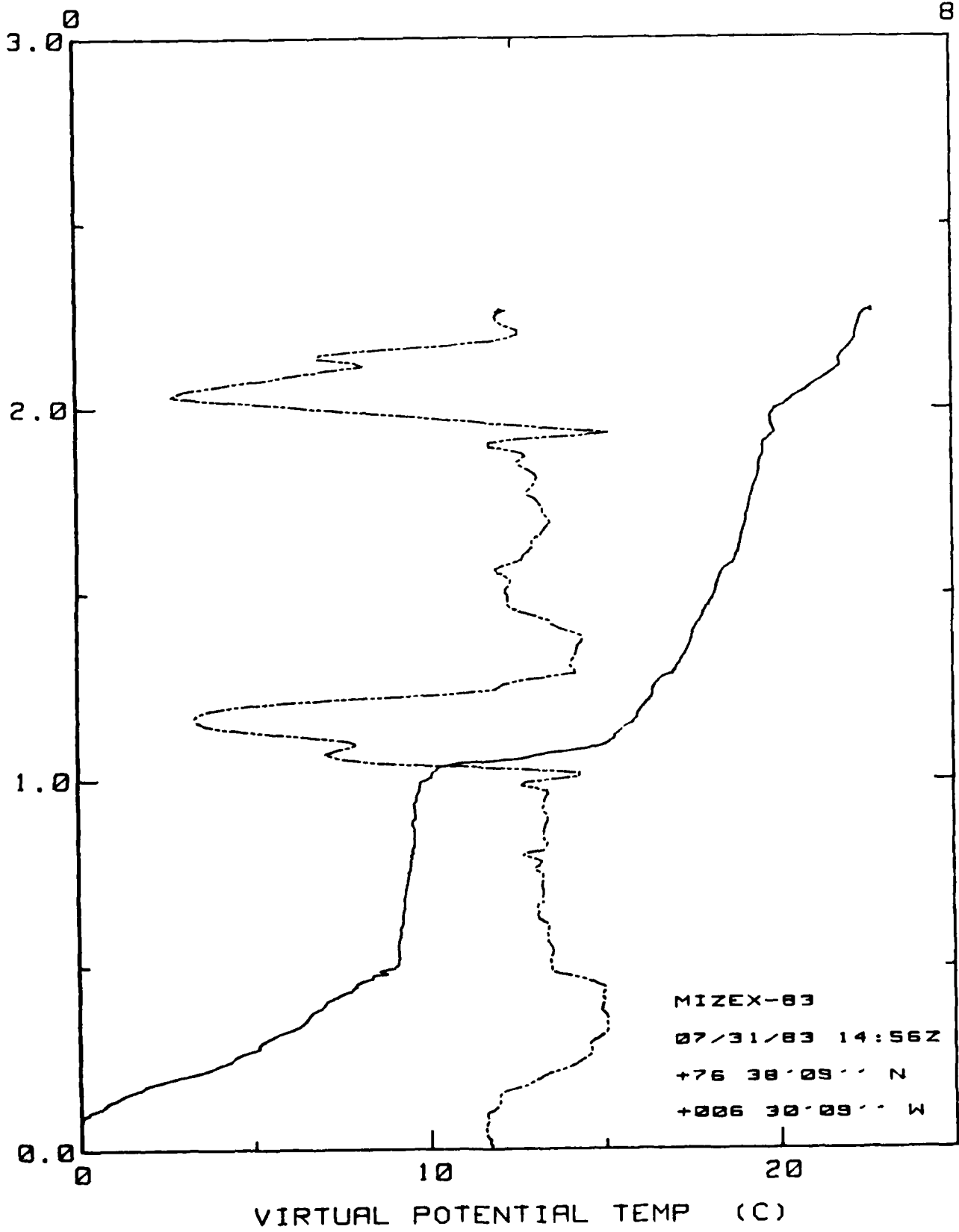
0 SPECIFIC HUMIDITY (g/Kg)



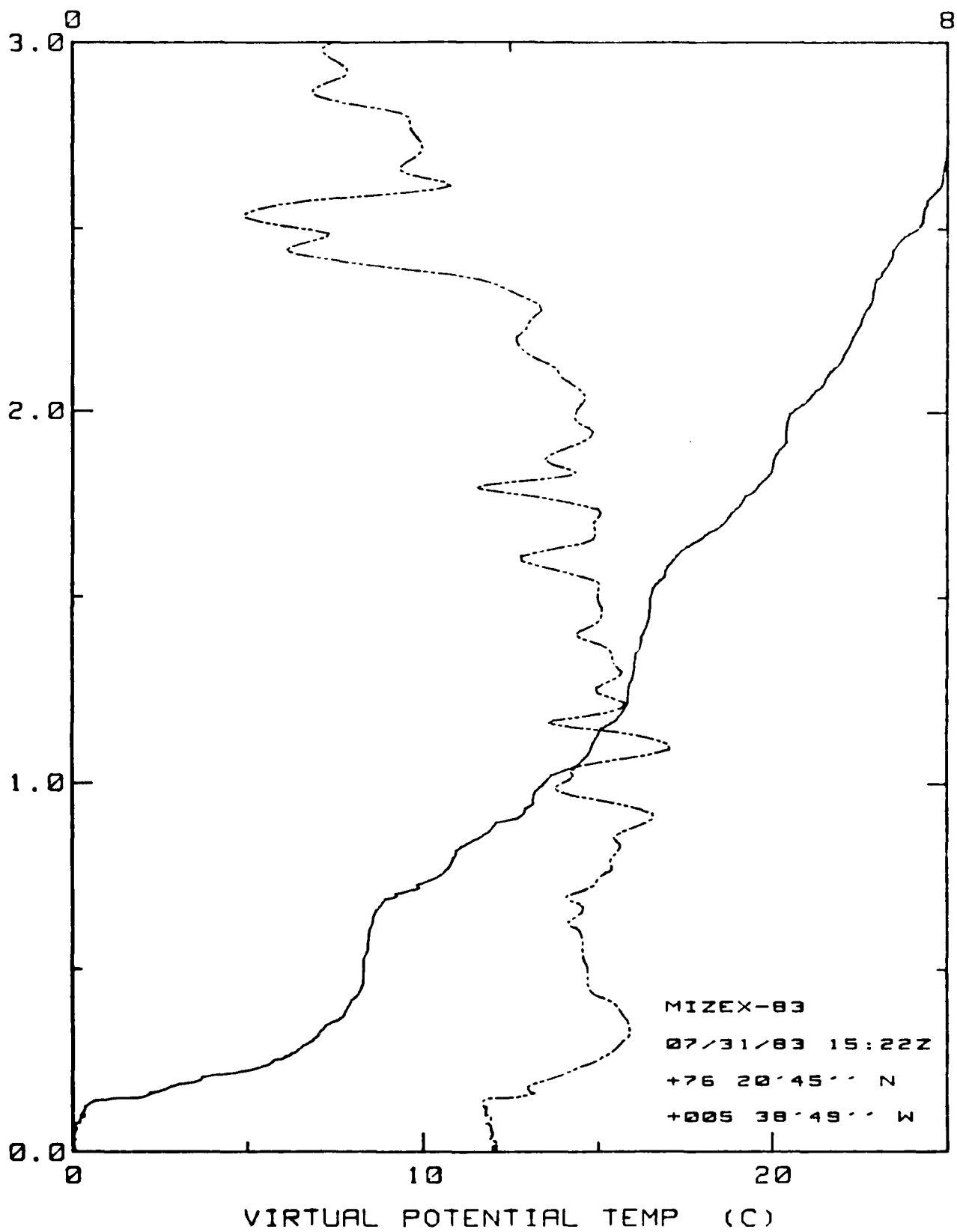
Q SPECIFIC HUMIDITY (g/Kg)



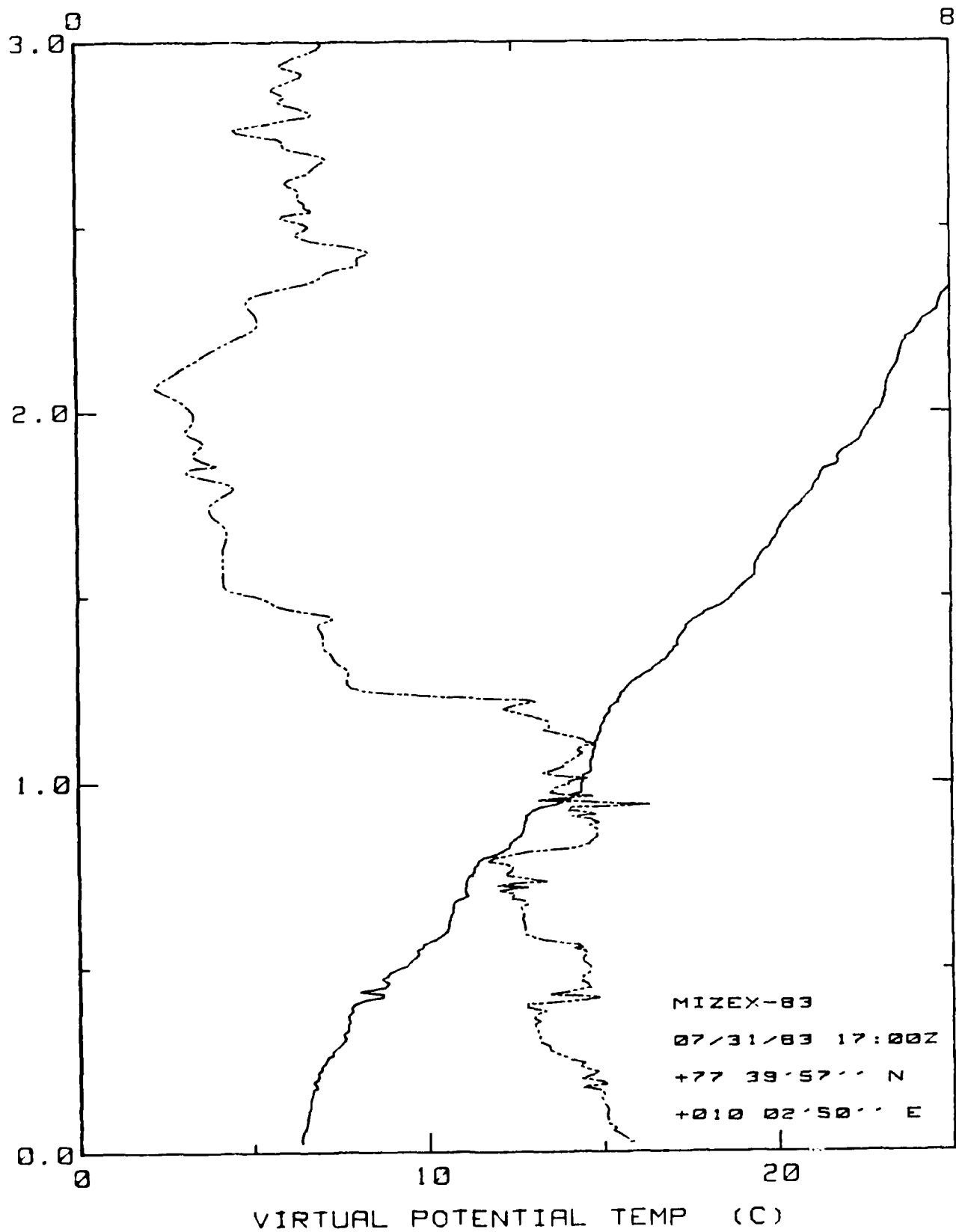
Q SPECIFIC HUMIDITY (g/Kg)



Q SPECIFIC HUMIDITY (g/Kg)



Q SPECIFIC HUMIDITY (g/Kg)



REPRODUCED

FILMED

8